Experimental Investigation and CFD modelling for Indoor Air Thermal Conditions in Worship Buildings in Egypt: Church and Masjid

Tarek A. Mouneer[1,*], Mohamed H. Aly[2], Ehab M. Mina[3]

[1] Mechanical Engineering Department, Benha Faculty of Engineering, Benha University.
[2] Mechanical Power Engineering Department, Faculty of Engineering, Helwan University.
[3] Mechanical Power Engineering Department, Faculty of Engineering, Ain Shams University.
*Corresponding Author e-mail: tarek.mouneer@bhit.bu.edu.eg, tarekadel2004@yahoo.com

ABSRACT:

Masjids and Churches are typical worship buildings constructed to serve citizens in Egypt since more over two thousands of years ago. This research classifies the methodology into three methods; i) experimental work, ii) Computational Fluid Dynamics (CFD), and iii) cooling loads analysis. The experiments were performed to measure the temperature distribution on both scaled down models for masjid and church, designed and constructed using 50:1 scale down ratio. Both models were tested at three loading conditions at 33%, 66%, and 100%. CFD modeling was performed to study flow filed of (MSJ-CFD) model with two configurations 1, 2, each at three different cases. The summative cooling load profiles give that only is presented on the connected load of common district cooling plant which dedicated to serve worship buildings consist of Masjid and Church. The comparison between results of both experimental and CFD investigations are in good agreement at their different locations and they give that the average air temperatures inside both experimental and CFD models at 19 ^{o}C for 33% load and Case 1, 22 ^{o}C for 66% load and Case 2, and 24 ^{o}C for 100 % load and Case 3, respectively. The results of summative cooling load profiles give that for maximum expected total load design for both buildings together design case can be reduced to 160 % of only one building of them, instead of 200% in normal standalone case. The conclusions are summarized to help decision making during planning and design stages either for Church or Masjid.

Keywords: church, masjid, mosque, praying area, thermal comfort, religious building, worship building, air conditioning.

NOMENCLATURE

g_i	gravity in x-direction	T_{avg}	Average Temperature, °C
H	enthalpy	t=0 min	t=0 min
h	Height in m	u	Velocity, m/s
l	Length in m	u_i	Velocity in x-direction, m/s
K	turbulence kinetic energy	u_j	Velocity in y-direction, m/s
k	thermal conductivity W/m.K.	$V_{sup.jet}$	Supply Air (Jetting) Velocity, m/s
p	Pressure	w	Width in m

Pr_k	turbulent Prandtl numbers for K	X	x-direction
Pr_ϵ	turbulent Prandtl numbers for ϵ	Y	y-direction
RH	Relative Humidity, %	Z	z-direction
T	Temperature, °C		

Greek Symbol

ε	dissipation rate
ρ	Density
μ	Viscosity

Subscripts

avg	average
i	unit vector in x-direction
j	unit vector in y-direction
K	turbulence kinetic energy
PVC	Polyvinyl chloride
sup	supply

Abbreviation

ACH	Air Change per hour
AHU	air handling unit
CFD	Computational Fluid Dynamics
CHU	Church
CU	Condensing Unit
C_n	Constant number n
EWH	Electrical Water Heater
MSJ	Masjid
T	Temperature Sensor

1. Introduction

Each building has its own occupancy pattern; places of worship are no exception. Despite generally low occupancy, worship places are designed to meet extreme design cases. Places of worship are key component in the urban plans of the new settlements adopted by the Egyptian government vision, "Egypt 2030 vision". This development vision includes the construction of at least 15 new settlements [1]. The New Capital, New Alameen City, New Mansoura City, New Minia, New Asyut, New Suez, and East Port-Said are examples of these "fourth generation cities" in the disclosed phase of the planed vision. The planned cities have a repeated urban block composed of one mosque and one church with common service facilities. Figure 1 compares between both types of worship buildings which are church building and masjid building to be included either at the New Capital or at any novel urban blocks in Egypt. Figures 1.a, and b show Christ Birth Church and Al-Fattah Al-Aleem Masjid, in New Capital in Egypt, respectively, in Birdseye views. Figures 1.c and d show typical church building and typical masjid building from inside, respectively.

(a) Christ Birth Church, New Capita100l, Egypt.

(b) Al-Fattah Al-Aleem Masjid, New Capital, Egypt.

(c) internal view for typical Church from inside.

(d) internal view for typical Masjid from inside.

Figure 1: Churches and Masjids, in both Birdseye views and external satellite views at New Capital in Egypt besides internal views, (a) Christ Birth Church, (b) Al-Fattah Al-Aleem Masjid, (c) typical church building from inside, and (d) typical Masjid building from inside.

A number of three groups are classified into three main categories of research interest which are the first group (Group I): conducted their researches on review, definition of parameters, applications of thermal comfort inside buildings [2-8], the second group (Group II): conducted their researches on churches architecture, thermal comfort, and energy efficiency either for heating or for cooling, [10-19], and the third group (Group III): investigated the mosques architecture, thermal comfort, and energy efficiency [20-34]. These three groups are classified in Table 1, which depicts each of these groups interests. Table 1 Classifies the literature into these three groups, besides classifies each of the second group of for churches buildings and third group for mosques buildings into three research interests which are thermal comfort, energy saving, and others interests such as acoustics studies, rehabilitation, and architecture designs. Table 1 depicts that many researches have been conducted on thermal comfort since 1970s by Fanger [2-3]. Most of these researches focused on thermal comfort inside different types of buildings [4-7]. A few numbers of these researches were conducted to study religious facilities [8-9], churches [10-19], and Masjids [20-34]. Some studies have been presented to predict the thermal comfort using dynamic similarity and CFD applications as one of most popular AC-systems design tools [35-39].

Table 1:
Classification of current literature review into three groups.

Group I: Thermal Comfort		**Group II: Churches Buildings**			**Group III: Mosques Buildings**		
Definitions & Fundamentals	**Religious Buildings**	**Thermal Comfort**	**Energy Saving**	**Other interests**	**Thermal Comfort**	**Energy Saving**	**Other interests**
Fanger [2], Fanger [3], Ricciardi & Buratti [4], Ricciardi et al. [5], Kwong et al. [6], Budaiwi [7].	Mushtaha & Helmi [8], Terrill & Rasmussen [9].	Hayati et al. [10], Muñoz-González et al. [11], Frasca et al. [12], Turcanu et al. [13], Vella et al. [14].	Aste et al. [15], Wessberg et al. [16].	Woroniak and Piotrowska-Woroniak [17], Rubeis et al. [18], Wang & Qu [19].	Saeed [20], Al-homoud et al. [21], Al-Ajmi [22], Abdullah et al. [23], Atmaca & Gedik [24], Azmi & Ibrahim [25].	Budaiwi et al. [26], Abdou et al. [27], Budaiwi [28], Ray et al. [29], Atmaca & Gedik [30], Azmi et al. [31].	Elkhateeb & Eldakdoky [32], Farrag [33], Shah [34].

Ricciardi and Buratti [4] have studied thermal comfort in the Fraschini theatre in Pavia, Italy. They presented the correlation between data from questionnaires, measurements, and mathematical model. Ricciardi et al. [5] investigated how to evaluate thermal comfort in an historical Italian opera theatre by the calculation of the neutral comfort temperature. Kwong et al. [6] presented a review study on thermal comfort assessment and potential for energy efficiency enhancement in modern tropical buildings. Budaiwi [7] presented an approach to investigate and remedy thermal comfort problems in buildings. Mushtaha and Helmi [8] has studied the Impact of building forms on thermal performance and thermal comfort conditions in religious buildings in hot climates: a case study in Sharjah city. Terrill et al. [9] presented an energy analysis of religious facilities in different climates through a long-term energy study. Terrill and Rasmussen [9] have evaluated HVAC energy usage and occupant comfort in religious facilities.

Several researches focused on the thermal performance and energy consumptions for church buildings either for heating or for cooling. Hayati et al. [10] investigated and modeled a single-sided ventilation through external doors, by measurements and model evaluation in five historical churches as they have stated. Muñoz-González et al. [11] presented Air conditioning and passive environmental techniques in historic churches in Mediterranean climate. A proposed method to assess damage risk and thermal comfort pre-intervention, simulation-based C. Frasca et al. [12] assessed the performance of hygrothermal modelling for diagnostics and conservation in an Italian historical church air change per hour. Turcanu et al. [13] investigated the optimal balance between cost management and thermal comfort for churches heating. Vella et al. [14] presented a study on thermal comfort in naturally ventilated churches in a Mediterranean climate. Aste et al. [15] presented sustainable church heating the Basilica di Collemaggio case study. Wessberg et al. [16] studied the feasibility of using the heat a long-term district heat demand forecast. They estimated the heating power and heat up time for intermittent on district heating and cooling heating of churches. Woroniak and Piotrowska-Woroniak [17] studied the effects of pollution reduction and energy consumption reduction in small churches located in Drohiczyn community. Rubeis et al. [18] studied thermal comfort and energy efficiency for severely damaged churches. Wang and Qu [19] focused the importance on the influence of Chinese and Western culture on modern church architecture in Yan' an area.

Several Researches focused on the thermal performance and energy consumptions for mosques (masjids). Saeed [20] demonstrated thermal comfort requirements in hot dry regions with special reference to Riyadh on Friday prayer. Al-Homoud et al. [21] presented an assessment of monitored energy use and thermal comfort conditions in mosques in hot-humid climates. Al-Ajmi [22] has studied thermal comfort in air-conditioned mosques in the dry desert climate. Abdullah et al. [23] defined thermal comfort control through urban mosque façade design. Recently, Atmaca and Gedik [24] evaluated thermal comfort and energy consumption inside mosques under temperate-humid climate. Azmi and Ibrahim [25] presented a comprehensive review on thermal performance and envelope thermal design of mosque buildings. Budaiwi et al. [26] investigated the envelope retrofit and air-conditioning operational strategies for reduced energy consumption in mosques in hot climates. Abdou et al. [27] evaluated the mosque energy performance by energy auditing using trends based on the analysis of utility billing

data. Budaiwi [28] has studied the envelope thermal design for energy savings in mosques in hot-humid climate. Ray et al. [29] have applied using design tools throughout the design process to intelligently controlled naturally ventilated mosque in their case study. Atmaca and Gedik [30] Determined thermal comfort of mosques in a temperate-humid climate using measurement and survey methods. Azmi et al. [31] focused on the factors influencing energy efficiency of mosque buildings. On the other hand, Elkhateeb and Eldakdoky [32] studied the acoustics of Mamluk masjids as a case study of Iwan-type masjids in Cairo, Egypt. Farrag [33] conducted a study on architecture of mosques and Islamic centers in Non-Muslim context. More recently, Shah [34] presents the possibility of opening of mosques in Pakistan for congregational prayers during Ramadan amid the COVID-19.

This literature reveals that neither any research has conducted on monitoring the energy saving in worship buildings consist of church and masjid in Egypt nor in any other country around the world. There is no research has been conducted on the idea of the benefits of grouping both worship buildings such as church and masjid together in the same urban block, neither experimentally nor numerically. For this reason, the current research question is raised in the author minds to present this comparative study between using experimental measurements and CFD, which extended to analytical study for cooling load profiles for both worship buildings.

This research investigates the total cooling loads required inside both of worship building (masjid and church) located in the same urban block at different load conditions. This paper is organized as follows: the following section, section 2, describes in detail the research methodologies using experimental work, CFD and cooling load analysis. The experimental work is presented in section 3 to indicate the details of experimental setup, instrumentation, and test procedures. Similarly, section 4 elaborates the details of the CFD simulation for a typical masjid as selected CFD model of the two worship buildings presented in the current study. Section 5 presents the experimental results, CFD results, and the results of the cooling loads. These evidences are organized together in the last section, section 6, to reach the paper conclusion and support the research message.

2. Research Methodology

In this section, the methodology of the current research is presented. This section is divided into three main parts which are: experimental setup and instrumentation, the CFD modeling techniques and its comparison with experimental results, and cooling load profiles for the two worship buildings located in the same urban block.

2.1 Experimental Work

Firstly, this research aims to perform experimental measurements for the temperature distribution inside both masjid experimental model (MSJ-model) and church experimental model (CHU-model). The supply and return air movement of Air conditioning (AC) system were carefully designed to build up these two experimental models and to ensure temperature uniformity inside both of these models. The air movement carries out the internal cooling loads due to the internal loads such as worshiper occupancy and internal lighting loads. A suitable

configuration of air distribution configurations has been proposed and selected to build up both models using supply and return air ducts of PVC pipes. An experimental test rig is described with the detailed designs aspects taken onto the two tested models, MSJ- model and CHU-model. The airside and system components are presented and their capacities are listed and tabulated. The measurements circuit and the used artificial loads have been described and the instrumentation accuracies are listed to detect the results accuracy upon. The details of experimental setup are presented in next section 3, however, the experimental results are presented later in section 5 as follows: subsection 5.1 for MSJ-model, and subsection 5.2 for CHU-model.

2.2 CFD Modelling

The second aim of this current research is to perform a particular simulation for heat transfer performance and thermal comfort inside one of the experimentally tested models which is MSJ-model, but using two different configurations of air distribution inside MSJ-CFD model by changing the level of air jet diffusers which are feeding the masjid space to carry out the expected and simulated internal cooling loads generated from both worshipers' occupancy and internal lighting system. A CFD commercial package of ANSYS Fluent was used to compute the flow domain upon the predetermined boundary conditions, mesh sizes, physical models for both of the tested configurations (Configuration A and Configuration B) for masjid CFD model (MSJ-CFD-model). The air velocities and temperature distributions are then presented to monitor and observe the effects of proposed air distribution on the thermal uniformity inside praying areas of numerically modeled masjid using CFD, and similar to that one experimentally tested in the first part of this research methodologies, as listed in the above subsection 2.1, and as will be described in details in next section 3. After that, a comparative study is presented between those experimental results of MSJ-model and these CFD results of MSJ-CFD-model. The CFD modelling details are presented in section 4, however, the CFD results and its comparison with experimental results are presented later in section 5, as follows: subsection 5.3 for MSJ-CFD-models results, and subsection 5.4 for comparison between experimental model MSJ-model and CFD model of Masjid MSJ-CFD-model.

2.3 Cooling Load Design Considerations

A typical cooling load profile for masjid building is predicated upon the daily and annual behavior of worshipers inside the masjid buildings for all prayers along the day hours and over the year occasions, and similarly a typical cooling load profile for church building is also predicted to thermally simulate the behavior of worshipers inside the church buildings for all prayers along the day hours and over the year occasions. Then these two cooling load profiles are added into one cooling load profile to simulate the third aim of this current research by buildup one chillers plant to serve the both worship buildings of church and masjid in the same urban block by summative techniques taking into consideration the diversity factors of each of these two buildings based on their own behavior in Egypt, and also taking into consideration the Egypt climate conditions and worshipers occupancies at different time periods of typical day, week, and along all the months of the year.

3. Experimental Work

Experimental work was performed to assess the influences of air distribution inside two scaled down model for both worship buildings consist of Masjid and Church located in the same urban plot plan. The two buildings were dynamically simulated using the two scaled down models clearly presented in this section. These two models were designed to be served from the same air side equipment as air handling unit (AHU) and also they are connected to the same refrigeration machine responsible for cooling process of these two models experimentally tested. This section describes the test rig in details, which consists of both models and their AC equipment which they equipped with. The measuring instrumentation and test procedures are listed in this section.

3.1 Experimental Setup Description

An experimental test rig was designed complete with two main parts; consist of both: masjid model (MSJ) and church model (CHU). Both of these two models MSJ and CHU are scaled down models for typical masjid with dimensions of L = 50 m x W = 50 m x H = 12 m, and for typical church with dimensions of L = 50 m x W = 50 m x H = 18 m, respectively. A scale down ratio was taken 50:1 for the three dimensions of typical masjid and typical church. A novel air distribution systems were used to supply air and to collect the return air inside MSJ-model and CHU-model. MSJ model and CHU model were equipped with air distribution systems consist of air ducts to carry out the expected internal loads such as people load and lighting load. The dynamic similarity techniques were used to build up the two experimental models, MSJ-model and CHU-model regarding to the scaled down ratio equal to 50:1. The dynamic similarity method was also used for internal heat generation term, to simulate and experimentally test the influences of air distribution, full load conditions, and part load conditions which are 33% and 66% of full load conditions, based on the varies worshipers' occupancies. Then, the optimal design of the air distribution was selected to monitor the air movements adjacent to the human bodies of worshipers at different vertical levels, to provide the intended thermal comfort inside these worship buildings Table 2 depicts the test rig system components and their dimensions, capacities either using equivalent number of prayers in the actual prototype for simulated masjid and church, or using the simulated cooling/heating artificial loads simulated in the test rig. Figures 2.a,b & c display the layouts for the test rig, CHU-model, and MSJ-model, respectively. The details and design aspect for bot CHU-model and MSJ-model are summarized in next subsection 3.1.1, however, the details of air side equipment and refrigeration machines used to provide the cooling loads for the test rig are listed in subsections 3.1.2. Then, the measuring instrumentations are specified in subsection 3.2.

3.1.1 MSJ-model and CHU-model

The dimensions of the two models of MSJ-model and CHU-model are shown in Figure 2-a. Meanwhile, Figures 2.b, c demonstrate the physical dimensions and the locations of temperature measurements for both models, CHU-model and MSJ-model, respectively. Each model construction is divided into three zones, while each zone has an electrical water heating element (EWH) with 1200 Watt, to simulate the internal loads of worshipers, by keeping

the temperature of water basin at 37 ± 1 °C. The walls and the roofs of both models, MSJ-model and CHU-model, are constructed using of acrylic boards with thickness of 4 mm for walls, and with thickness of 3 mm for roofs. A LED lighting elements were attached to the roof of each model during testing to simulate the internal lighting loads inside the masjids and churches during praying times. Figures 3 depicts several Birdseye views and end views for both of the tested models, MSJ-model and CHU-model.

Table 2:
Test Rig Main Components Specifications.

	MSJ-model	CHU-model	Air Handling Unit (AHU)	Condensing Unit (CU)
Model Dimensions				
Length (mm)	1000	1000	450	500
Width (mm)	1000	600	500	500
Height (mm)	300	500	450	450
Occupancy				
Total Number of Persons (Person/sq. meter)	0.6	0.5	N/A	N/A
Expected person No. (person)	3500	3000	3500 for MSJ 3000 for CHU	3500 for MSJ 3000 for CHU
Artificial Loads/ Cooling Loads (Watt) or (hp)	EWH Load = 1200 W No. of EWH = 3 Total Load = 3600 W	EWH Load = 1200 W No. of EWH = 3 Total Load = 3600 W	Cooling coil =360 W Air Flow = 0.1 m^3/s	Comp.= 1/8 hp

Key

1. **CHU-model**
2. **MSJ-model**
3. **Supply Air Ducts**
4. **Return Air Ducts**
5. **Electrical Water Heaters (EWH).**
6. **Temperature Sensors (T).**
7. **Air Handling Unit (AHU).**
8. **Condensation Unit (CU)**
9. **Pipes with diameters (63 mm, 50 mm, 40 mm, 32 mm)**
10. **Tees *Tees and one elbow work as Air diffusers**
11. **Valves (Ball valve)**
12. **Elbows**

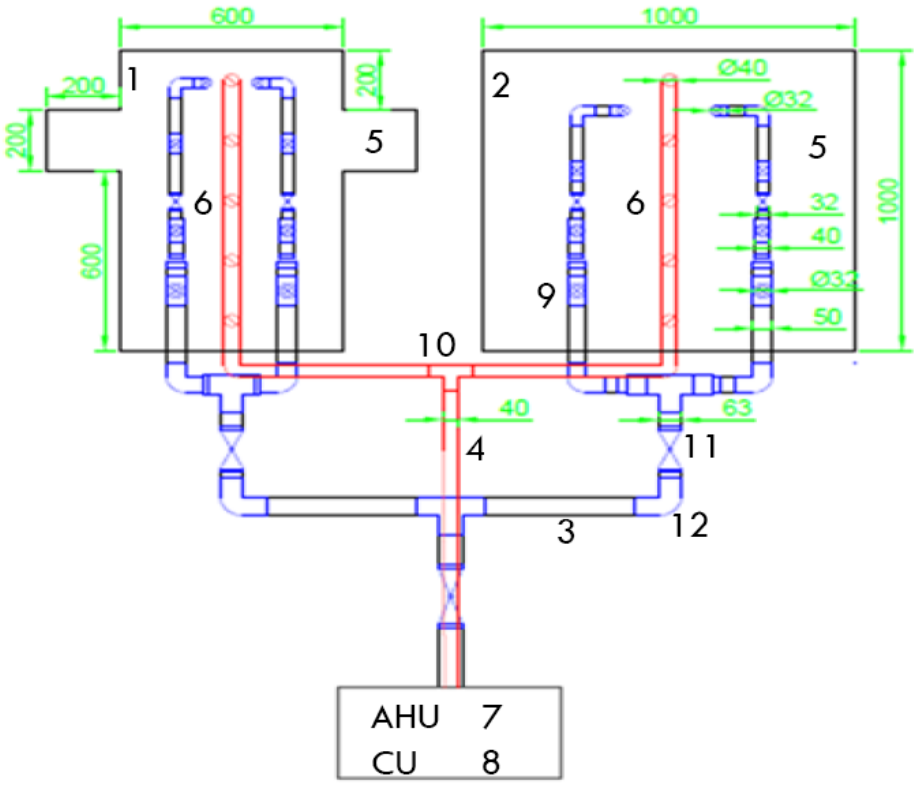

(a) Schematic layout for experimental test rig consists of CHU-model, MSJ-model, and air handling equipment (AHU).

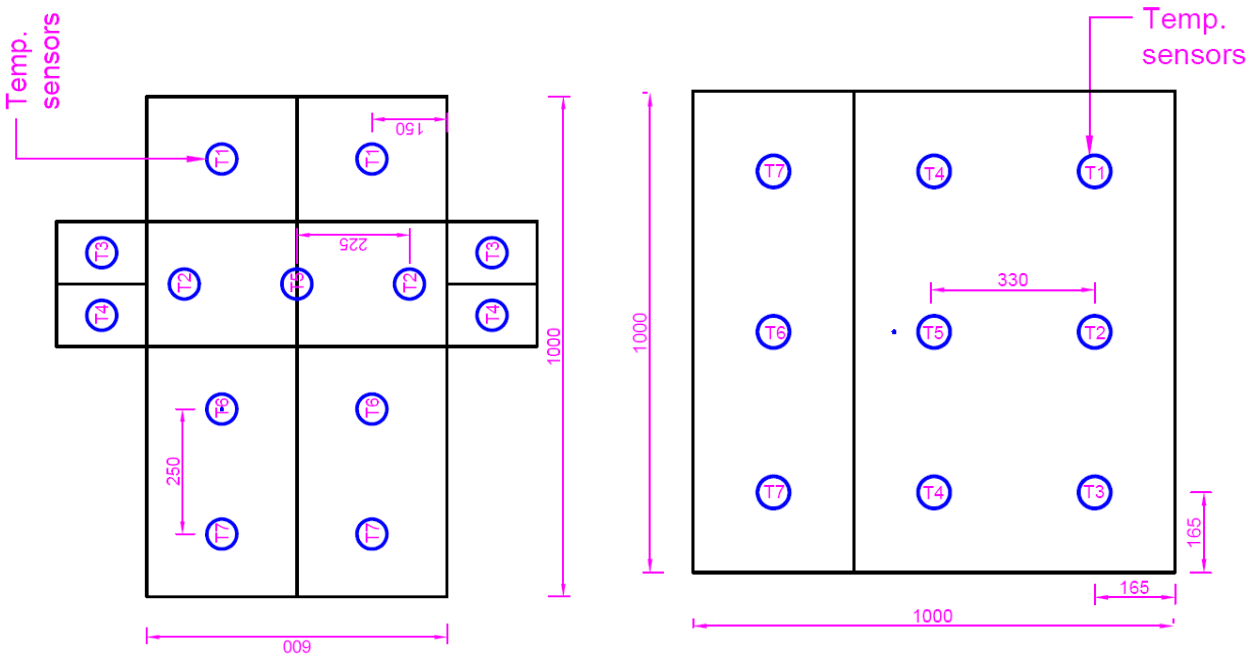

(b) dimensions of CHU-model (c) dimensions of MSJ-model.

Figure 2: Schematic diagrams for test rig layout and the two experimentally tested models CHU-model and MSJ-model, (a) test rig layout, (b) temperature sensors locations of CHU-model, and (c) temperature sensors locations of MSJ-model.

Figure 3: Experimental setup for test rig consists of two tested models MSJ-model and CHU-model, End view for test rig consists of MSJ-model (on left side), CHU-model (on right side), and AHU the back connected to refrigeration machine of air cooled condensing unit (CU).

3.1.2 Air Side Equipment, Air Distribution Ducts and Refrigeration Machine

To perform the current experimental work an Air handling unit (AHU), with specified dimensions and capacity listed in Table 2, was carefully designed and constructed as can be seen in Figure 4-a for the AHU from inside including cooling coil and air blower, and as also can be seen in Figure 4-b for the AHU from outside connected to the main supply air duct and main return air duct. An air cooled condensing unit (CU) is used as main source

of refrigeration used to provide the cooling capacity demand of the AHU cooling coil. The test rig is equipped with air distribution system consists of supply and return air ductwork. The ductwork serves as a pathway for the transportation of the air from the AHU to and from the conditioned space(s). Rigid Polyvinyl chloride (PVC) pipes were selected to perform the current research experimental work as supply and return air ducts for airflow. Rigid PVC pipes is very hard with specified temperature resistance up to 130 °C and low thermal conductivity which is approximately K=0.8 W/m.K. PVC pipes have low internal surface roughness approximately 0.02 mm. Figure 4-b shows the used PVC piping system used to connect the AHU to both models as the main supply air duct and main return air duct.

3.1.3 Measurements Instrumentation and Artificial Loads

Two types of temperature sensors were used for temperature measurements inside both tested models, MSJ-model and CHU-model. The two types of temperature sensors are digital panel type. The first is insert design type (TPM-900), and it can work in operating environment with temperature range: 0 °C ~ 60°C, and environment humidity range between RH=20% ~ 85%. TPM-900 uses power supply of 220VAC±10%, with power consumption less than 3 Watts per sensor. The displaying resolution is 0.1 °C for temperatures less than <100 °C, and 1°C for temperature higher than ≥100° C. It is equipped LCD display as can be seen in Figure 5-a. However, the second type is insert design type (TPM-10) with temperature range between -50°C~+100°C, using environment temperature -5°C~+50°C, and humidity is 5%~80%. The recorded accuracy is ±1°C for this type with resolution of 0.1°C. The Power can be provided by two button battery (LR44, 1.5v). Figure 5-b shows the second type of temperature sensor (TPM-10). Table 3 depicts the technical data for the used temperature sensors. Each of the tested models, CHU-model and MSJ-model, are equipped with three e electrical water heater each with power =1.2 kW, current = 20 Ampere, voltage = 220 volt, and each element is controlled with thermostat of range from 20 to 80 °C. Figure 5-c shows the used electrical water heater (EWH) used to simulate the internal people loads, as artificial loads with 3 steps heater each of 1.2 kW, with total heating capacity of 3.6 kW which can simulate the different prayer occupancy. Figure 5 displays the experimental apparatus and procedures used to investigate air temperature and movement inside the two experimentally tested models MSJ-model and CHU-models.

Table 3:
Temperature sensors specifications

Sensor Type		Accuracy	Capacity/ Range
Temperature Sensors (TPM-900)	Type A	0.1 ºC	displaying range = 300+110°C Power supply= 220VAC ±10% < 3W
Temperature sensors (TPM-10)	Type B	0.1 ºC	-50°C~+100°C RH= 5% ~ 80%

(a) AHU from inside **(b)** AHU from outside

Figure 4: Experimental Apparatus used to supply Air and to measure air temperatures onside the two tested models MSJ and CHU, (a) AHU from inside consists of cooling coil, and air blower, (b) AHU from outside connected to air distribution system.

a) Temperature sensor Ttype A accuracy 0.1 ºC.

(b) Temperature sensor tType B accuracy 0.1 ºC.

(c) Water Electrical heater (EWH) with thermostat.

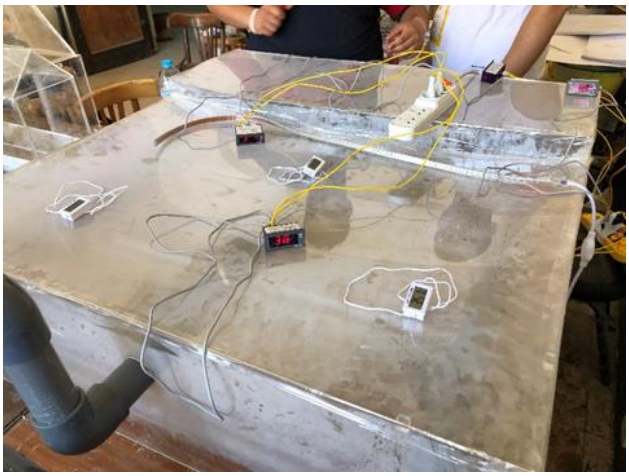

(d) Temperature sensors installed on MSJ model from outside.

(e) AHU from outside and air distribution system of supply & return air ducts.

Figure 5: Experimental Apparatus and Procedures for the two tested models MSJ and CHU (a) Temperature sensor type A, (b) Temperature sensor type B, and (c) electrical water heater (EWH), (d) MSJ-model from outside and installed temperature sensors, (e) MSJ-model from inside and air distribution system of supply and return air ducts, and Water Electrical heater (EWH).

3.2 Experimental Procedures

A set of experiments have been performed to study the heat transfer performance inside the two built up models, MSJ-model and CHU-model by monitoring the temperature distributions inside both models during the cool down period. A set of historical temperature curves are plotted to assess the thermal performance and to evaluate the effect of air distribution on the thermal comfort for worshipers at different locations inside the tested model. The historical temperature curves are plotted using the temperature measurements at full load condition (3 x 1.2 kW = 3.6 kW) is started at time t=0 min where T=35 ^{o}C and end at time t= 210 min at T = 17 ^{o}C, which is the desired space air temperature. These experiments for each model are repeated at 33% of full load, and 66% of full load. A selective set of this experimental data for full load conditions are presented in section 5 of results and discussion. The part loads experiments are in good agreement with those of full load, however, for data reduction purpose only the full load condition experiments are demonstrated in this article. Figure 5 displays the experimental procedures used to investigate air temperature and movement inside the two tested MSJ-model and CHU-model. Figure 5-d shows the MSJ-model from outside and the installed temperature sensors, however, Figure 5-e shows MSJ-model from inside and air distribution system of supply and return air ducts, and water electrical heater (EWH).

4. CFD Modelling

Several researches conducting computational fluid dynamics (CFD) modelling as one of commonly used numerical tools by air conditioning system designers to numerically investigate the thermal behavior, temperature uniformity to avoid hot spot problems, and the influence of air distribution on flow field inside nonresidential buildings during different stages of air conditioning design process. Yi and Feng [36] investigated dynamic integration between building energy simulation (BES) and CFD simulation for building exterior surface. Fan et al. [37] studied the coupled simulation of BES-CFD and performance assessment of energy recovery ventilation system for office model. Fan and Ito [38] have studied integrated building energy computational fluid dynamics simulation for estimating the energy-saving effect of energy recovery ventilator with CO_2 demand-controlled ventilation system in office space. Sørensen and Nielsen [39] presented the quality control of computational fluid dynamics in indoor environments. Youssef et al. [40] conducted CFD study to evaluate the performance of cold air system inside a 2D space. They studied the flow of cold air at different supply temperatures, velocities, and room thermal loads. They calculated the effective return air temperature by using the results of velocity field and the temperature distribution inside the studied space.

4.1 Numerical Experiments Setup

A few number of numerical experiments has been set up to demonstrate the importance preliminary CFD investigations which are mostly dedicated to gain a deep understanding for the thermal uniformity, and the thermal

comfort and environment inside masjid building with two different air distribution configurations using air jet diffusers. Three two different configurations of air jetting are designed and investigated, with the following Configurations: Configuration 1 with air jets at level Y= 4 m, and Configuration 2 with air jets at level Y=14 m. However, the total height of the numerically tested CFD models are kept at 18-meter-high, similar to one of the firstly built masjids in New capital which is used to carry out the current CFD study included in the current work. Each of these two air jetting configurations, is tested with using a number of 12 air jet diffusers at two levels, (Y=4 m, and Y=14 m) for MSJ-CFD-model. The total mass flow rate of supplied air into the numerically tested masjid model is kept constant in both investigated experiments, as listed in Table 4. Figure 6 demonstrates the two models designed in the current research to simulate both worship buildings under current investigation of Masjid and church buildings. However, the masjid CFD model (MSJ-CFD-model) using CFD software package is displayed in Figure 6-a, and church 3D model (CHU-CFD-model) complete with proposed supply air ducts at two different levels using solid works software package is shown in Figure 6-b.

Table 4:

Classification and specifications of numerical setup program for both current work and future work.

CFD models /Configurations	Dimensions (mm)	Supply Air inlet height m	Total Number of Persons	Present work or Future work	Artificial Loads/ Cooling Loads Watt
MSJ-CFD-model Configuration 1	L=30 m W=40 m H=18 m	14	3500	present work	Peoples load kept at 37 ^{o}C Lighting Load = 20 W/m^2
MSJ-CFD-model Configuration 2	L=30 m W=40 m H=18 m	4	3500	present work	Peoples load kept at 37 ^{o}C Lighting Load = 20 W/m^2
CHU- CFD-model Configuration 3	L=50 m W=30 m H=18 m	14	3000	recommended future work	Peoples load kept at 37 ^{o}C Lighting Load = 20 W/m^2
CHU- CFD-model Configuration 4	L=50 m W=30 m H=18 m	4	3000	recommended future work	Peoples load kept at 37 ^{o}C Lighting Load = 20 W/m^2

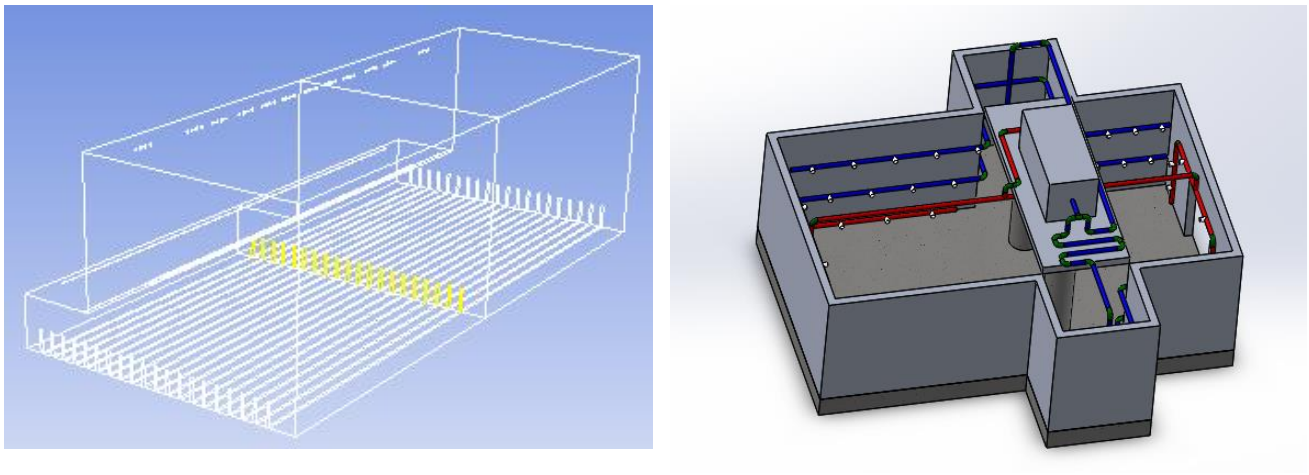

(a) MSJ-CFD model using ANSYS Fluent **(b)** CHU-model using solid works

Figure 6: 3D Views for MSJ-CFD model CHU-CFD model tested in the current research (a) MSJ-CFD model using ANSYS Fluent software package, (b) CHU model using solid works software package.

4.2 Physical Model

In the present three-dimensional CFD investigation, two models are designed and modeled, then their results can be presented in the next Results and Discussion section, in subsection 5.3. These numerically tested models can be classified into two configurations (Configuration 1 and Configuration 2) for MSJ-CFD model based on the level of supply air jetting inside the MSJ-CFD models. The air are supplied into both of these MSJ-CFD models by 12 air jet diffusers installed at two different levels as can be seen in both Figures 7-a,b, at 14 meter height for configuration 1, and at 4 meter height for configuration 2, respectively. The MSJ-CFD models external dimensions, which are taken as (40 m x 30 m x 18 m) for both Configurations 1 and 2. Figure 7-c shows all views (elevation, plan, side view, and isometric views) for CHU-CFD model to be simulated and numerically investigate on the same concept of studying the influence of supply air jetting on thermal uniformity and thermal comfort for worshippers inside churches. Figure 7-d illustrate the cross pattern for CHU-CFD model in complete model plan view. Figure 7-e displays the CHU-CFD model in half church model to reduce processing time and computing processes. The worshippers heat loads are the greatest term of internal loads upon worshippers' occupancies at different operating time inside each of the worship buildings, of church and masjid.

The mesh generated and imported into flow field using both commercial CFD software package of Gambit, and Ansys Fluent for both CFD models, MSJ-CFD model Configuration 1, and MSJ-CFD model Configuration 2. This software has been commonly used by many authors to detect the thermal behavior inside buildings and spaces inside it using CFD analysis. Ansys Fluent was early recognized and considered as powerful simulation tool for thermal behavior, heat transfer performance either in cooling or heating conditions. Besides, the heat load of peoples either in constant heat fluxes or in constant temperature surfaces. The current physical models were used the constant temperature method to account the internal people loads inside MSJ-CFD model by keeping their surface temperatures at 37 ^{o}C, similar to the same experimental conditions used for the experimental setup

presented in the current research to facilitate comparison between both expected results from MSJ-model experimentally tested as described in previous section 3, and MSJ-CFD model numerically tested as described below in this section 4. This software produces highly accurate, conformal meshes that represent the true shape of internal load components. The three-dimensional MSJ-CFD models (Configurations 1 and 2) are simulated on ANSYS Fluent 7.0 as shown in Figure 7-a, b. Each of simulated worship temperature was kept fixed at 37 ^{o}C for all computational run for both of the tested configurations 1 and 2. The supply inlet air temperature (T_{in}) from the supply air jet diffusers to the praying hall of MSG-CFD model was kept at 18 ^{o}C. This temperature range is in a good agreement with those experimentally investigated used for the experimental setup presented in the current research to facilitate comparison between both results from MSJ-model experimentally tested and MSJ-CFD model numerically tested. The height of both models (H) used for Configurations 1 and 2 is kept H=18 meters height, however to study the influence of air jetting levels on the thermal comfort enhancement the air jetting levels are changed at two levels, which are the height is kept H=14 meters for Configuration 1, and the height is kept H=4 meters for Configuration 2. After the supplied air entering the praying hall to carry out their people loads and any other dissipated heat loads, its temperature rises, and then become as returned air leaving the praying halls through the return air outlets designed in MSJ-CFD model with both configurations 1 and 2. Figure 7 depicts the physical models for MSG-CFD model using ANSYS Fluent software and for CHU-CFD model using Solid works software.

4.3 Governing Equations

In the present study, three-dimensional model is considered, where the flow of air in both models are considered unsteady, turbulent, and incompressible. The characteristics of the air flow are obtained by solving the Navier-Stokes and energy equations. The system mathematical model is formed as follows:

Continuity equation:

$$\frac{\partial \rho}{\partial t} + \partial_i(\rho u_i) = 0 \qquad \text{Equation (1)}$$

Momentum equation:

$$\frac{\partial (\rho u)}{\partial t} + \partial_j\left(\rho\, u_i\, u_j\right) = \mu \partial_{jj} u_i - \partial_i p + \rho g_i + S_i \qquad \text{Equation (2)}$$

Energy equation:

$$\frac{\partial (\rho H)}{\partial t} + \partial_i(\rho\, u_i H) = \partial_i(K\, \partial_i\, T) \qquad \text{Equation (3)}$$

The time scale and turbulent length are estimated by solving the transport equations of the turbulent model. Standard K- $\boldsymbol{\epsilon}$ model is used for turbulence kinetic energy (K) and dissipation rate ($\boldsymbol{\epsilon}$) as following.

$$\frac{\partial(\rho K)}{\partial t} + \frac{\partial}{\partial x_i}(\rho\, k\, u_i) = \frac{\partial}{\partial x_i}\left[\left(\mu + \frac{\mu_t}{Pr_k}\right)\frac{\partial k}{\partial x_j}\right] + P_k + P_b - \rho\epsilon - Y_M + S_k \qquad \text{Equation (4)}$$

$$\frac{\partial(\rho\epsilon)}{\partial t} + \frac{\partial}{\partial x_i}(\rho\, \epsilon\, u_i) = \frac{\partial}{\partial x_i}\left[\left(\mu + \frac{\mu_t}{Pr_\epsilon}\right)\frac{\partial \epsilon}{\partial x_j}\right] + C_1\frac{\epsilon}{k}(P_k + C_3P_b) - C_2\rho\frac{\epsilon^2}{k} + S_e \qquad \text{Equation (5)}$$

where, Pr_k and Pr_{ϵ} are turbulent Prandtl numbers for K and ϵ and, respectively, and P_b and P_k are turbulence kinetic energy generations due to buoyancy and velocity gradient, respectively. S_K, and S_e are source terms, Y_M is the fluctuating dilatation to the overall dissipation rate in the turbulence contribution, and finally, C_1, C_2, and C_3 are constants.

4.4 Numerical Simulation Technique

Computational Fluid Dynamics (CFD) is becoming a powerful tool in modeling flow field and temperature distribution in worship building; this is due to The high cost of performing experiments. By using the CFD model, airflow distribution and its thermal profile are simulated in the masjid and church, in addition to assisting the designer in identifying the performance of cooling system and preferable location of air outlet to obtain the best distribution of air stream. The first step of this work is pre-processing, in which the geometry is defined and grid generation step where the domain is divided into small cells at which the governing equations are solved, this is done here using ANSYS Fluent software. The second step involves solving the equations (Conservation of mass – Momentum- Energy – K-ε) for each cell, using finite volume method and selecting ANSYS-Fluent as a solver. The turbulence of airflow and PCM phase change is also solved numerically by applying k-ϵ while the pressure correction of the conservation equations is performed by applying SIMPLE scheme. Values of 0.1, 0.2, 0.7, and 1 are considered for the under relation impact of density, pressure, momentum, and thermal energy, respectively. Then, post-processing step where the results are presented using graphic tools such as temperature contours and velocity vectors in addition to calculating performance parameters indices, knowing that the solution must achieve convergence criteria. The mesh size is selected to satisfying convergence criteria of 10^{-6} for the continuity, 10^{-8} for the momentum, and 10^{-12} for the energy equations, and 10^{-8} for K- ϵ model. The boundary conditions for performed numerical experiments of the tested models are listed in Table 5.

Table 5: Boundary conditions for MSJ-CFD models numerically tested for both configurations 1 and 2.

CFD models /Configurations	Internal wall temp. °C Suppl	Persons Surface Temp. °C	Supply Air Temp. °C	Supply Air Flow rate m^3/s		Supply Air (Jetting) Velocity m/s
MSJ-CFD-model Configuration 1	3333	37	17	(ACH=2) (ACH=1) (ACH=0.5)	0.340 0.170 0.085	3.8 1.8 0.9
MSJ-CFD-model Configuration 2	333	37	17	(ACH=2) (ACH=1) (ACH=0.5)	0.340 0.170 0.085	3.8 1.8 0.9

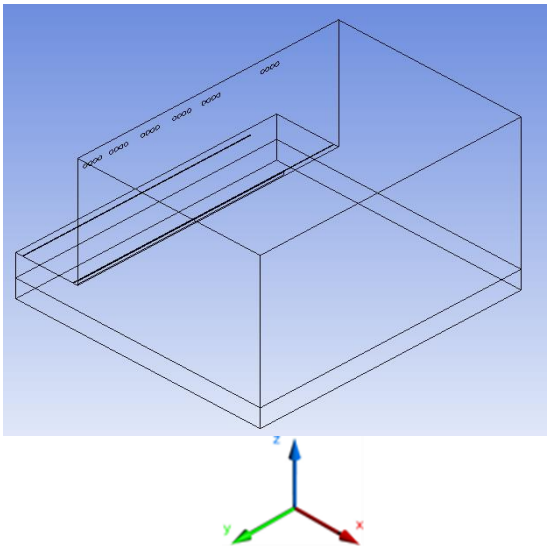

a) MSJ-CFD-Model - Configuration 1

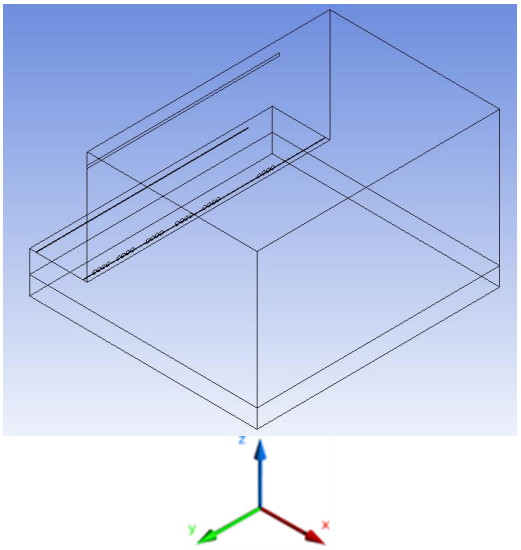

b) MSJ-CFD-Model - Configuration 2

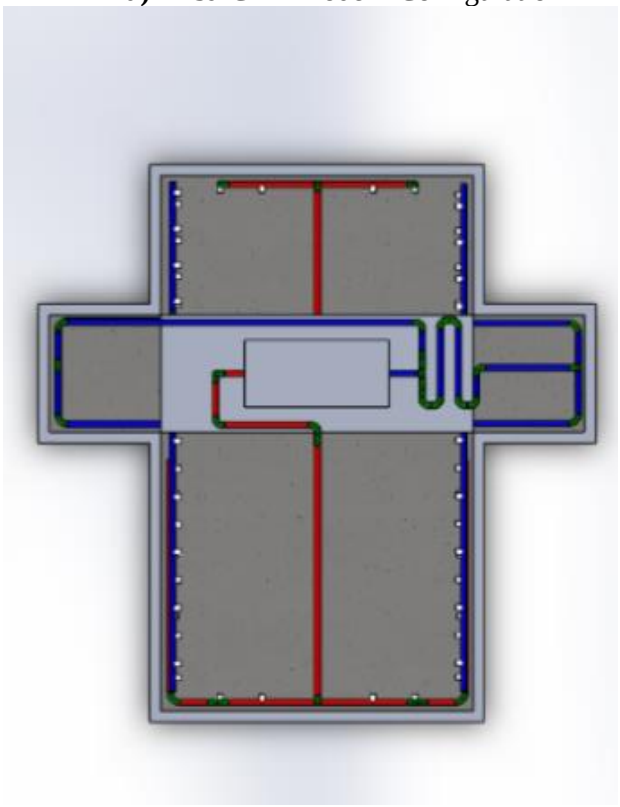

c) CHU-Model in plan view

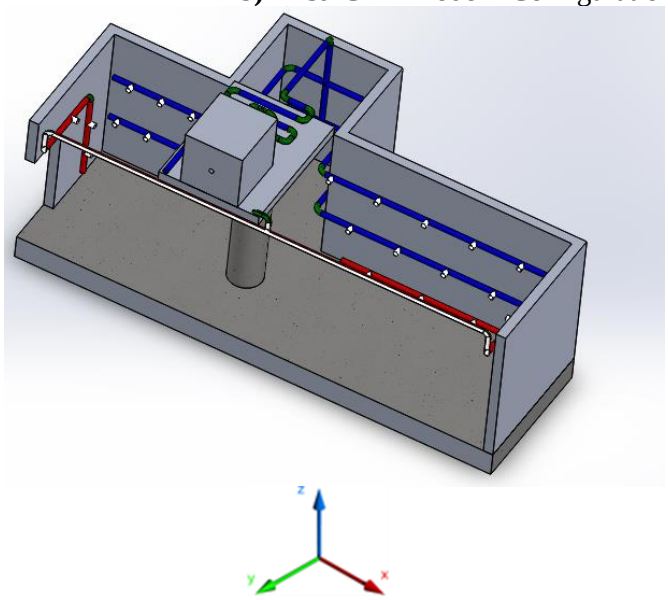

d) CHU- Model in three dimensional view

Figure 7: Physical Models for both CFD models; MSG-CFD model using ANSYS Fluent software and CHU-CFD model using Solid works software a) MSG-CFD model Configuration 1, b) MSG-CFD model Configuration 2, c) Plan view for CHU-model in cross pattern, and d) half model to simulated for CHU-CFD model with two supply air jetting levels, recommended for future work.

4.5 Mesh Independence Study

The grid generation step is very important as the structured mesh makes the solution faster and the solution gets convergence easier. In the present three-dimensional CFD study, fine mesh for the domain has been carefully generated to solve the model with the optimum number of cells, which gives better results and consumes the shorter processing time. Mesh independence study with six different number of cells starts from 1,000,000 cells and up to 5,400,000 cells has been detected before starting the current CFD investigation on the two tested configurations. Table 6 depicts the results obtained for mesh independency test performed on MSJ0CFD model – Configuration 1, in the preliminary tests to validate the constructed CFD model for MSJ-CFD model independent on its grid sizes, as can be observed in Table 6. Table 6 reveals that both the average praying hall temperature and its average velocity starting to be stabilized after the number of 4,800,000 grid size until 5,400,000 grid size of the MSJ-CFD model configuration 1.

Table 6: Mesh Independency study for CFD Simulations for one of MSJ-CFD model numerically tested for both configurations 1.

CFD models /Configuration	Number of Cells	Average praying Hall Temp. °C	Average praying hall Velocity m/s
MSJ-CFD-model Configuration 1	1 060 000	13	0.05
MSJ-CFD-model Configuration 1	1 750 000	17.5	0.07
MSJ-CFD-model Configuration 1	2 450 000	19.25	0.08
MSJ-CFD-model Configuration 1	3 800 000	20.50	0.1
MSJ-CFD-model Configuration 1	4 800 000	22.5	0.12
MSJ-CFD-model Configuration 1	5 400 000	21.5	0.11

4.6 CFD Model validation study associated with experimental model

The validation for CFD model has been performed to validate the CFD results using the current software package, and then it can be discussed to study their impacts on the decision making for air conditioning system design for these types of worship buildings, such as Masjid and Church. One of the numerically tested configuration for MSJ-CFD model was carefully compared with those results measured on geometrical similarly configuration of Masjid. The results of these comparative and validation study are presented in Figure 8, for MSJ-CFD model

Configuration 1, and MSJ-validation experimental prototype model, which has been constructed using the experimental apparatus and test rig, experimentally tested for Masjid in this current research. The comparison gives a good agreement between the CFD results generated using current software code, and those experimentally measured on the preliminary model constructed to simulate the CFD-MSJ model, with the same dimensional ratios in the three dimensions. Both models, CFD-MSJ and MSJ-validation, are included the cavity contains below Women praying area which is commonly located in Mezzanine Floor Level, as can be seen on both Figures for both models, CFD-MSJ (Figures 10 and 11) and MSJ-validation (Figures 5.d and 5.e), respectively.

Figure 8 illustrates the experimentally measured supply air temperature and average temperatures in three different zones inside MSJ-validation model, which divided into three zones; frontal zone, intermediate zone, and rear zone of the masjid. However, the numerically investigated CFD results for MSJ-CFD model gives their average temperature in the same three zones as classified in the experimental validation model MSJ-validation model are identical. These average temperatures can be clearly observed in temperature distribution inside MSJ-CFD model configuration 1, as can be seen in Figure 11, discussed in the next sections. Figure 8 indicates the slightly observed and commonly expected deviations between both CFD result, and validation experimental model results. Figure 8 confirms on the validity of the used CFD software to numerically investigate the thermal behavior and velocity investigations using this CFD technique, presented in section 4 for CFD results performed in this current study. The preliminary results of numerically generated CFD model for MSJ with configuration 1 for the average temperatures, presented in Table 6, are in good agreement with those average temperatures experimentally recorded after the steady state condition has been reached, as can be seen in Figure 8 for the performed preliminary experiment on MSJ-experimental model, which is geometrically similar to that one of MSJ-CFD configuration 1, as shown in Figure 8, This this validation study findings verify and can enough validate the CFD results to be generated in current study.

5. Results and Discussion

This section demonstrates both types of the experimental and CFD results investigated in the current research to monitor the thermal comfort inside different kinds of worship buildings in Egypt consist of church and masjid. The results are classified into three subsections which is identical to those classified above in the research methodologies and objectives which are can be classified as following: i) experimental results in subsections 5.1 such MSJ-model results is listed in subsection 5.1.1, and CHU-model results is listed in subsection 5.1.2 for, ii) CFD results is listed subsection 5.2, and iii) the results of summative cooling load profiles analysis for simultaneously operation pf both worship buildings of masjid and church in the same urban plan which are similar to those early presented in section 1 of current research introduction.

5.1 Experimental Results for Historical Temperature Curves for MSJ model and CHU model

In the current experimental study, the set of experimental results underwent a reduction in data to present a selective experimental measurement for historical temperature profiles for both models of MSJ-model and CHU-model which were experimentally investigated. Figure 8.a depicts the historical temperature curves, versus experiment duration time of 210 minute (3.5 hours) performed in typical day of July day data inside MSJ-Model. Figure 8-a displays the supply air temperature and temperatures measurements monitored at the seven locations dedicated for temperature sensors, as can be seen in Figure 2-c. These temperatures were measured using the temperature measurements device at the seven locations, as can be seen in Figure 2-c for MSJ-model. These locations are normally distributed to detect the thermal behavior in all of the internal zones of the masjid, which were classified into three thermal comfort zones up on the occupancy of the worshipers at different praying times and day of the week either Fridays or other typical prayers in all of the week days except Fridays. Meanwhile, Figure 8.b displays the historical temperature curves, versus experiment duration time of 210 minute (3.5 hours) performed in typical day of July day data inside CHU-Model. Figure 8.b illustrates the supply air temperature and temperatures measurements monitored at the seven locations dedicated for temperature sensors, as can be seen in Figure 2-b. These temperatures were measured using the temperature measurements device at the seven locations, as can be seen in Figure 2-b for CHU-model. These locations are normally distributed to detect the thermal behavior in all of the internal zones of the church, which were classified into three thermal comfort zones up on the occupancy of the worshipers at different praying times and day of the week either Sundays or other typical prayers in all of the week days except Sundays.

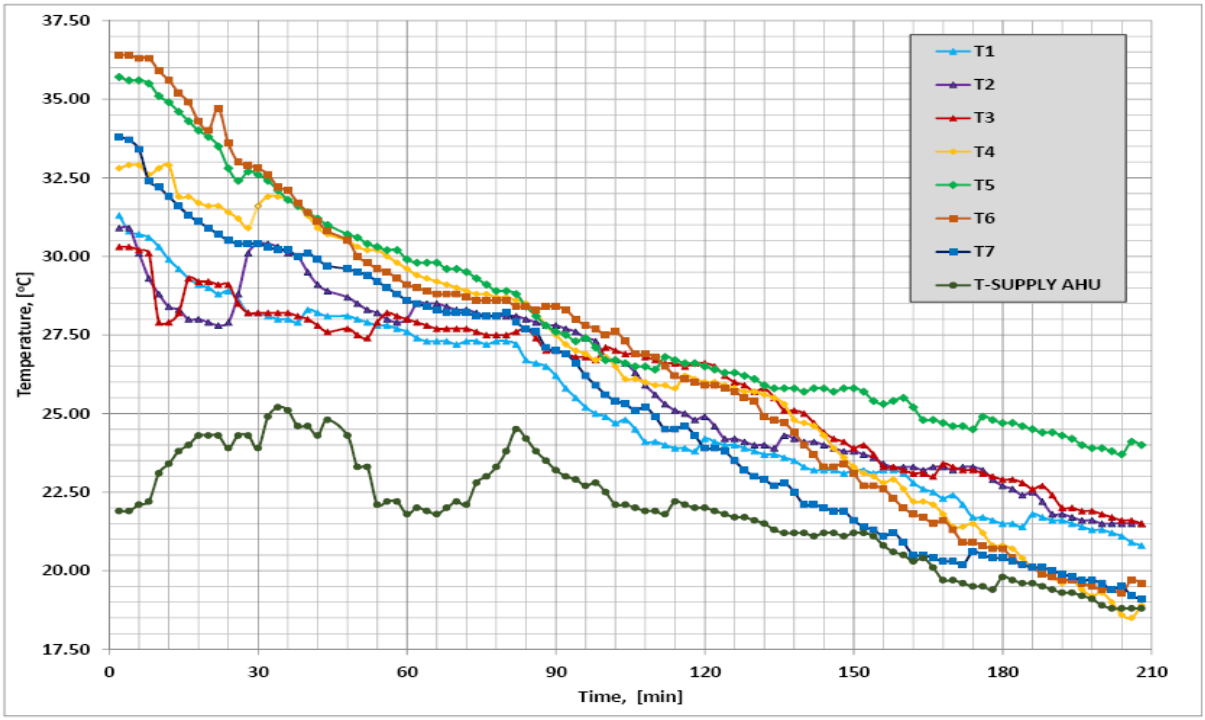

(a)

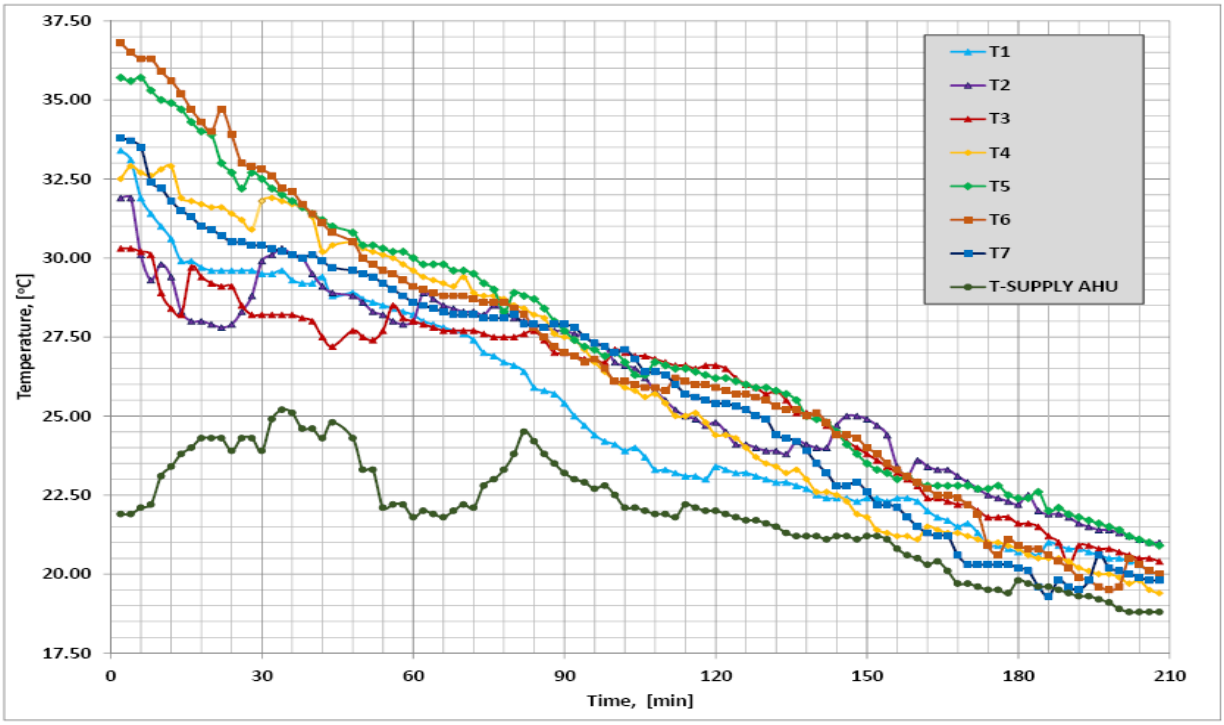

(b)

Figure 8: Historical Temperature Curves versus Time for 3.5 hours experiments performed in typical July day data. for supply air temperature and temperature measured in 7 locations. a) inside MSJ-Model, and b) inside CHU-Model.

5.2 CFD Results for MSJ-CFD model for both configurations

5.2.1 Velocity Magnitudes and Distribution for MSJ-CFD-model with two configurations

Figure 9 demonstrates the velocity magnitudes shown on both vertical median Planes and horizontal Planes at worship head levels for MSJ-CFD-model configurations which are: Configuration 1 - Case 1 and for Configuration 2 –Case 2. Figure 9-a displays the velocity magnitudes on vertical median Plane of the masjid model at Z=20 m, for Configuration 1 with Case 1. The figure shows that the supply air jetting level is taken at high level at Y= 14 meter, as listed before in Tables 4 and 5 describe the configuration 1 geometry and boundary conditions. The supply air velocity from the 12 air jet diffusers installed at Y =14 meter appears to be within value of 3.8 m/s, as indicated for Case 1 of both of the tested configuration as depicted in Table 5. Then the air is distributed from this high level to reach to the praying hall at prayers head level at Y= 1.8 m. Figure 9-b displays the velocity magnitudes on vertical median plane of the masjid model at Z=20 m, for Configuration 2 with Case 3. The figure shows that the supply air jetting level is taken at high level at Y= 4 meter, as listed before in Tables 4 and 5 describe the configuration 2 geometry and boundary conditions. The supply air velocity from the 12 air jet diffusers installed at Y =4 meter appears to be within value of 1.0 m/s, as indicated for Case 3 of both of the tested configuration as depicted in Table 5. Therefore, the air is easily distributed from this level and rapidly reach to the praying hall at prayers head level at Y= 1.8 m. It should be clear that Figure 10 Compares between the

velocity magnitudes for both configurations 1 and 2, with two cases 1 and 3 respectively, which are selected after CFD data reduction strategy in current research. In this data reduction technique the authors selected to present the better performance of all the generated computational runs for both of the CFD tested configurations for MSJ-model, under the boundary conditions for three numerically investigated cases with different supply air jetting velocity as depicted before from Table 5.

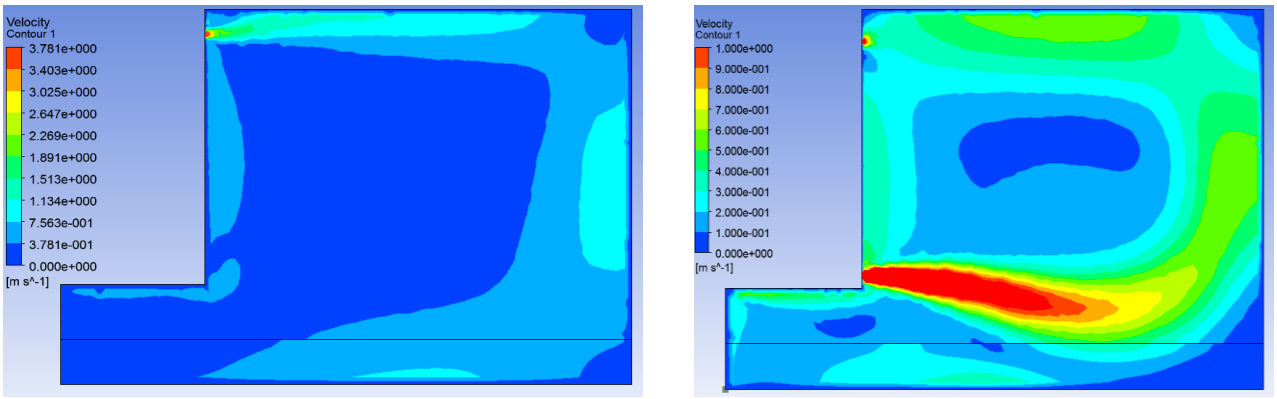

a) **b)**

Figure 9: Comparison of velocity magnitudes for both configurations of MSJ-CFD-model, Configuration 1 and Configuration 2, shown on vertical sectional at middle of Masjid CFD model at Z=20 m. a) MSJ CFD Model Configuration 1-Case 1, b) MSJ CFD Model Configuration 2 - Case 3.

5.2.2 Temperature Distribution for MSJ-CFD-model with two configurations

Figure 10 displays the temperature distribution inside MSJ-CFD-model, with both configurations Configuration 1 and Configuration 2, on a set of vertical and horizontal planes. Figures 10-a and b illustrate the temperature distribution on vertical median plane at the middle of the MSJ-CFD model at Z=20 m for both configurations: Configuration 1, case 1, and Configuration 2, case 3, respectively. For deep understanding the temperature distribution on a set of vertical planes at different locations for one of the tested MSJ-CFD configuration, Figure 11 displays the temperature distribution on a set of vertical planes at different Z-values for MSJ-CFD-model Configuration 1 – Case 1, where Figure 11-a at Z=20 m (which is at the middle of the masjid model), Figure 11-b at Z=15 m, Figure 11-c at Z=10 m, and Figure 11-d at Z= 5 m. Figure 12 depicts the temperature distribution on horizontal plane views at different Y-levels for both configurations of MSJ-CFD-model, Configuration 1 – Case 1 and Configuration 2 – case 3. Figures 12-a and c display the temperature distribution for configuration 1 – case 1 on horizontal planes at Y=14 m, and at Y=10 m respectively. However, Figures 12-b and d display the temperature distribution for configuration 2 – case 3 on horizontal planes at Y=4 m, and at Y=2 m respectively. Figure 12-e displays the velocity magnitudes for Configuration 1 with Case 1 on horizontal Plane at Y=1.8 m, which is approximately equivalent to prayers head level. Figure 12-f displays the velocity magnitudes for Configuration 2 with Case 3 on horizontal plane at Y=1.8 m, which is approximately equivalent to prayers head level.

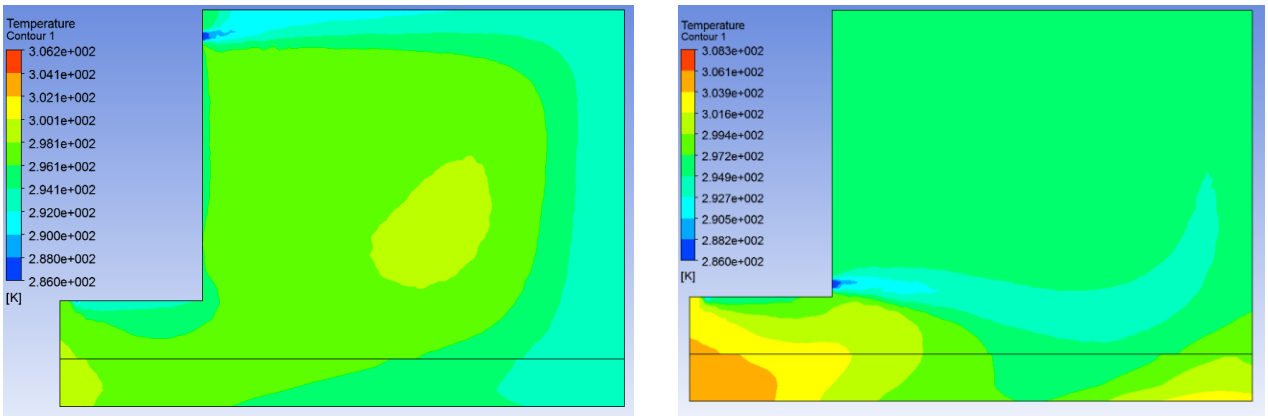

a) **b)**

Figure 10: Temperature Distribution for both configurations of MSJ-CFD-model, Configuration 1- case 1 and Configuration 2- case 3 shown on vertical middle sectional views at Z=20 m, at middle of Mas-CFD model. a) MSJ CFD Model 1 -Vertical median plane at Z=20 m, Case 1. b) MSJ CFD Model 2 -Vertical median plane at Z=20 m, Case 3.

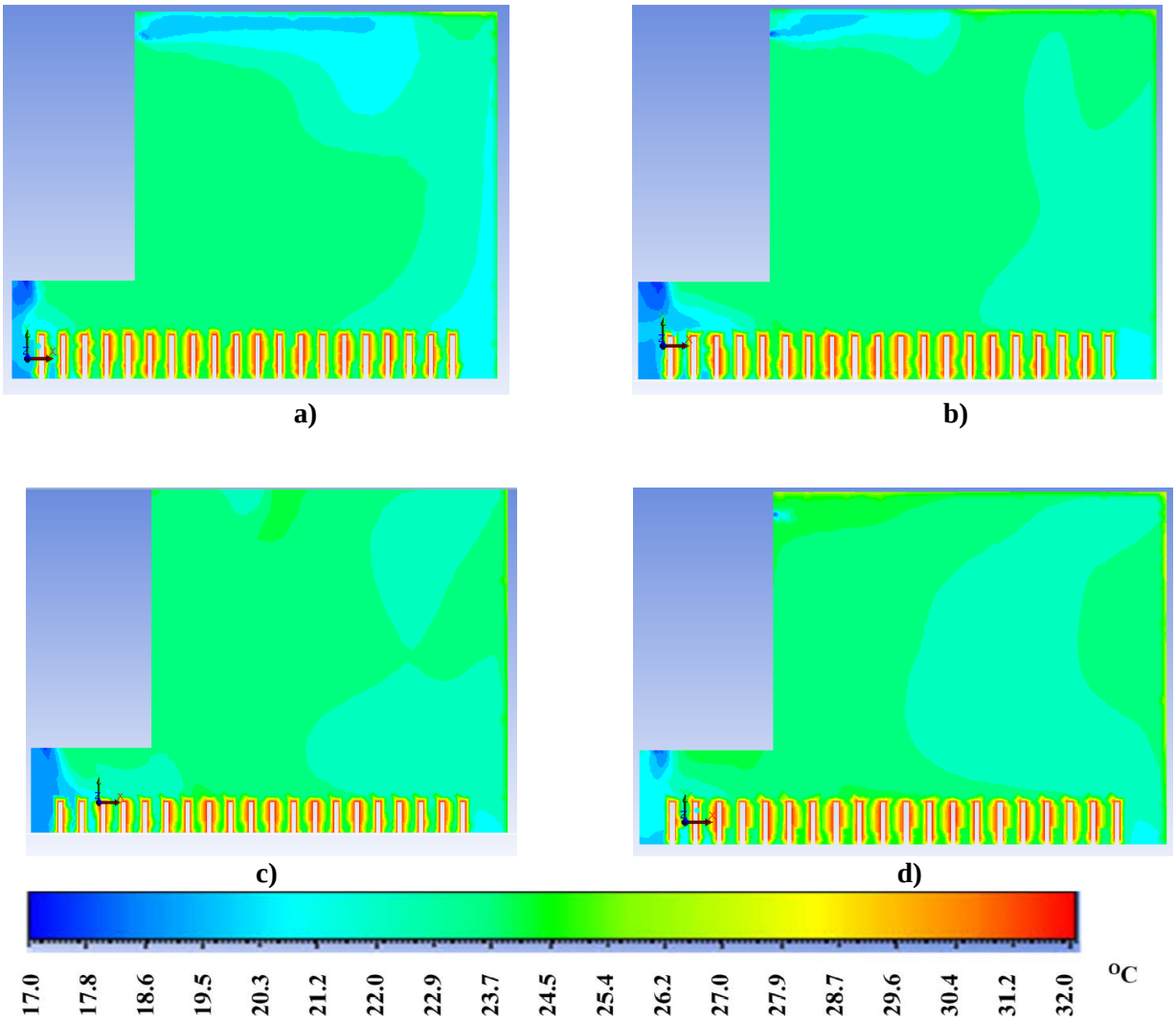

a) **b)** **c)** **d)**

Figure 11: Temperature Distribution for both configurations of MSJ-CFD-model Configuration 1- case 1 shown on vertical sectional views at different Z-values. a) Z = 20 m, b) Z= 15 m, c) Z = 10m, and d) Z=5 m.

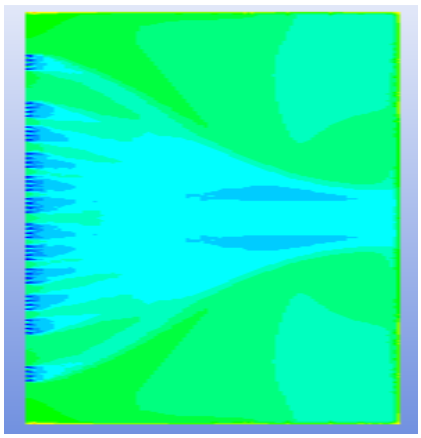

a) Tempreture distribution at y=14 m

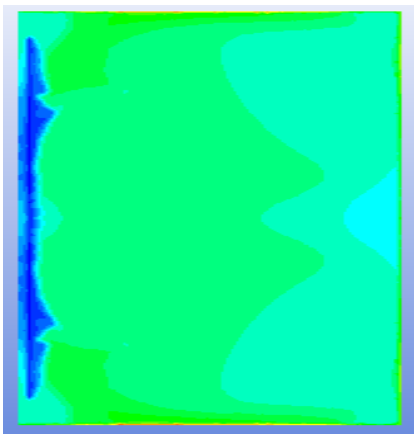

b) Tempreture distribution at y=4 m

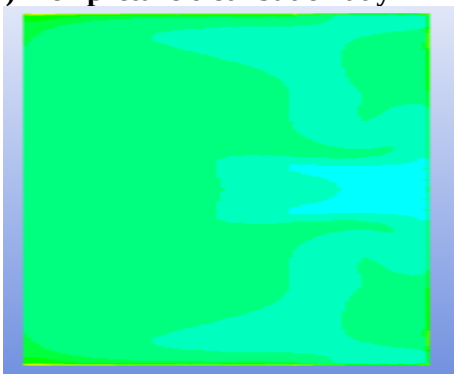

c) Tempreture distribution at y=10 m

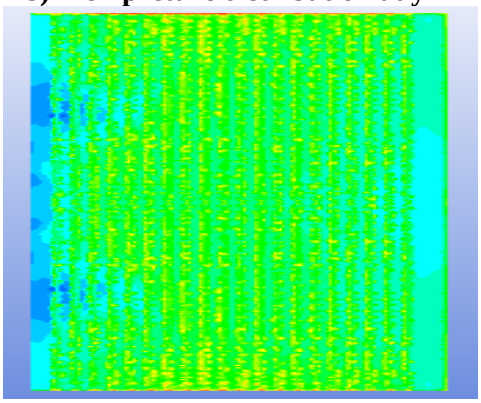

d) Tempreture distribution at y=2 m

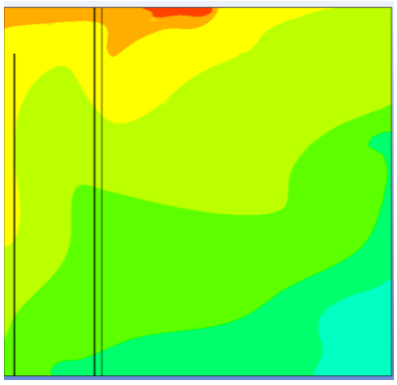

e) Horizontal plane at worshipers head level at Y =1.8 m, Case 1.

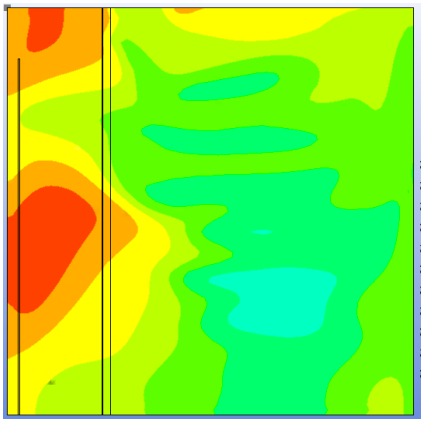

f) Horizontal plane at worshipers head level at Y =1.8 m, Case 3.

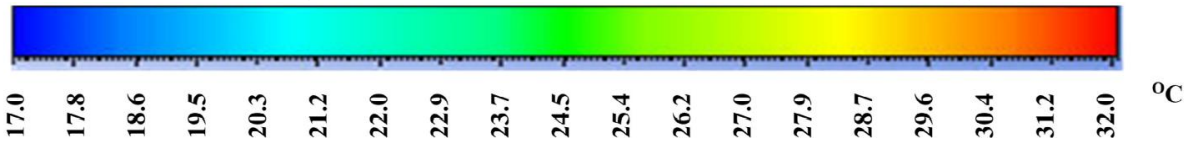

Figure 12: Temperature Distribution on horizontal plane views at different Y-levels for both configurations of MSJ-CFD-model, Configuration 1 and Configuration 2, a) horizontal plane for configuration 1 at Y=14 m, b)

horizontal plane for configuration 2 at Y=4 m, c) horizontal plane for configuration 1 at Y=10 m, and d) horizontal plane for configuration 2 at Y=2 m.

5.3 Comparison between Experimental and CFD Results for MSJ-model

Figure 13 demonstrate the average temperature measurements performed inside MSJ-validation model, for supply air temperature and temperature average for three zones (front, middle, and rear). These averaging results have been investigated based on those several temperature sensors, as presented in Figures 8-a, b. Figure 14 displays the comparison between temperature distributions experimentally measured on MSJ-experimental model at middle level horizontal plan views, with those numerically generated by CFD model for MSJ-CFD models Configuration 1 with three cases 1, 2, and 3. Figure 14.a depicts the good agreement observed between the temperature measurements and results by the used CFD package for the MSJ experimental at 33% Loading and the MSJ-CFD model Configuration 1, Case 1. Similarly, Figure 14.b gives the identity between temperature distributions for both experimental and CFD models, which are the MSJ experimental at 66% Loading and the MSJ-CFD model Configuration 1, Case 2. However, Figure 14.c depicts the good agreement between the experimental and numerically investigated temperature measurements for both investigated models in this current research, which are the MSJ experimental model at 100% Loading and the MSJ-CFD model Configuration 1, Case 3.

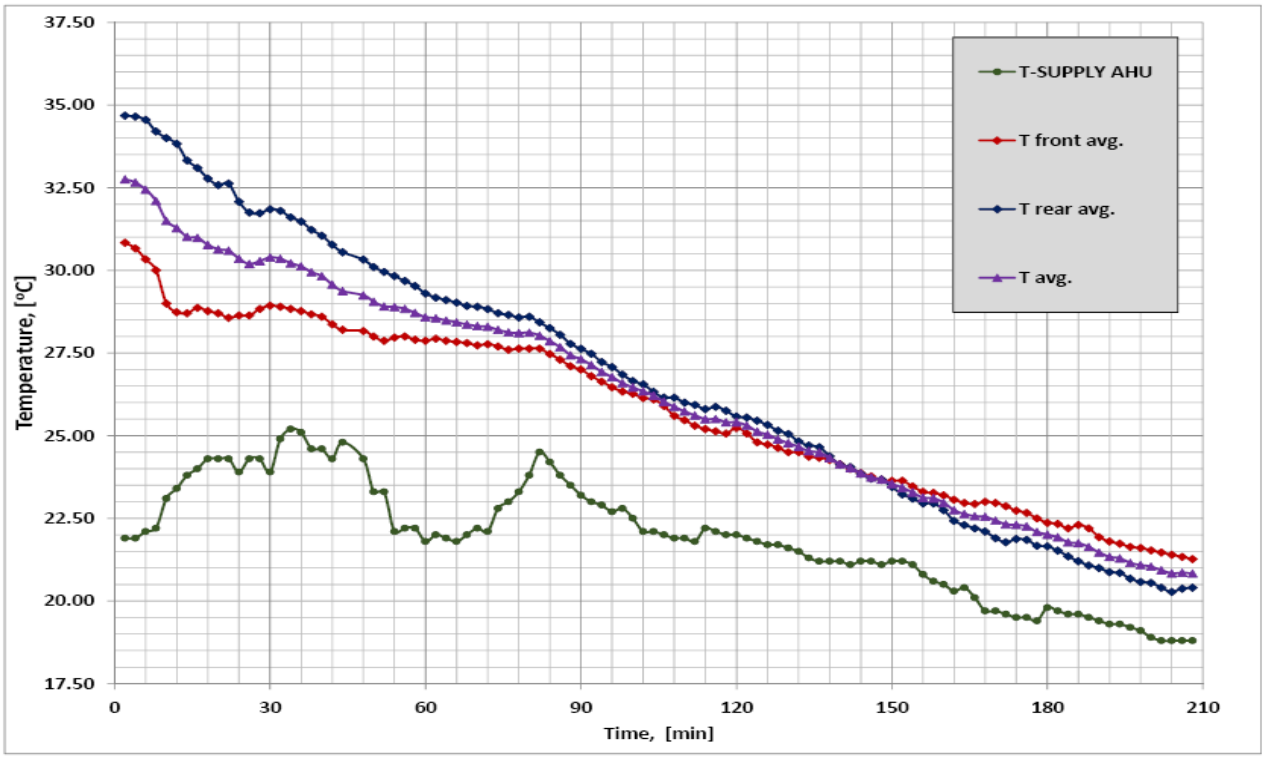

Figure 13: Average Temperature Measurements performed inside MSJ-validation model, for supply air temperature and temperature average for three zones (front, middle, and rear).

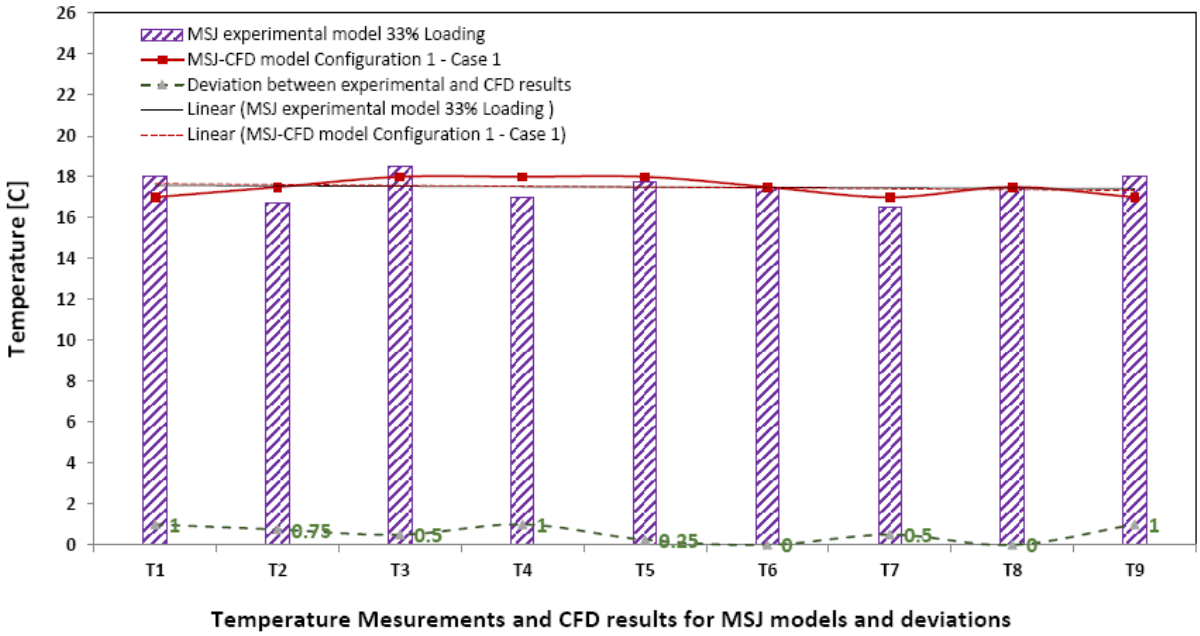
MSJ experimental model 33% Loading
MSJ-CFD model Configuration 1 - Case 1
Deviation between experimental and CFD results
Linear (MSJ experimental model 33% Loading)
Linear (MSJ-CFD model Configuration 1 - Case 1)
Temperature [C]
T1
T2
T3
T4
T5
T6
T7
T8
T9
1
0.75
0.5
1
0.25
0
0.5
0
1
Temperature Mesurements and CFD results for MSJ models and deviations

a

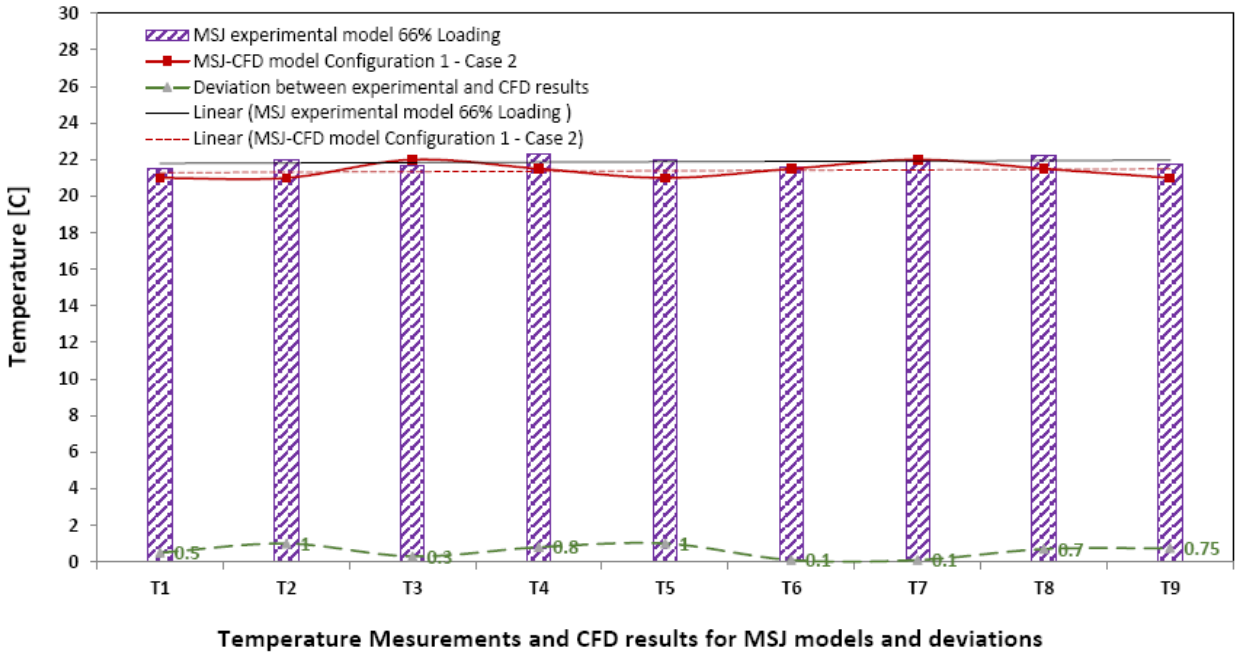
MSJ experimental model 66% Loading
MSJ-CFD model Configuration 1 - Case 2
Deviation between experimental and CFD results
Linear (MSJ experimental model 66% Loading)
Linear (MSJ-CFD model Configuration 1 - Case 2)
Temperature [C]
T1
T2
T3
T4
T5
T6
T7
T8
T9
0.5
1
0.3
0.8
1
0.1
0.1
0.7
0.75
Temperature Mesurements and CFD results for MSJ models and deviations

b

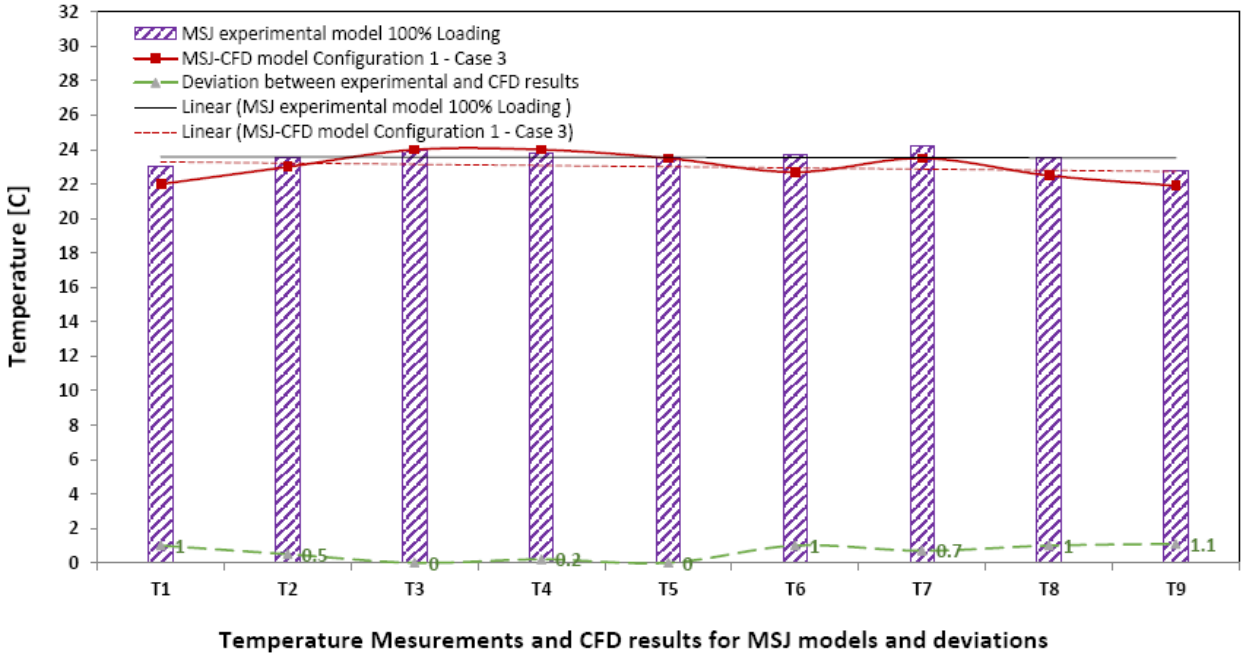

c

Figure 14: Comparison between experimental against MSJ-CFD model temperature distributions measured on MSJ-experimental model with three loading at middle level horizontal plan view, with those computed by for MSJ-CFD model Configuration 1 with three cases. a) MSJ Configuration 1, Case 1, at 33% Loading b) MSJ Configuration 1, Case 2 at 66% Loading, and c) MSJ Configuration 1, Case 3 at 100% Loading.

5.4 Results of Summative Cooling Load Profiles for MSJ and CHU buildings

A typical cooling load profile for masjid building is predicated upon the daily and annual behavior of worshipers inside the masjid buildings for all prayers along the day hours and over the year occasions, and similarly a typical cooling load profile for church building is also predicted to thermally simulate the behavior of worshipers inside the church buildings for all prayers along the day hours and over the year occasions. Then these two cooling load profiles are added into one cooling load profile to simulate the third aim of this current research by buildup one chillers plant to serve the both worship buildings of church and masjid in the same urban block by summative techniques taking into consideration the diversity factors of each of these two buildings based on their own behavior in Egypt, and also taking into consideration the Egypt climate conditions and worshipers occupancies at different time periods of typical day, week, and along all the months of the year. Figure 14 depicts the cooling load profiles for Masjid, Church and total for both buildings for different typical holidays of Fridays, Sundays, Ramadan and Feasts, a) Typical Friday in July, b) Typical Sunday in July, and c) typical Ramadan/feast day in July. Besides, Figure 14 displays depicts the Satellite Views for Typical arrangements for existing Masjid and Church in the same urban plot in two different locations in Nasr City zone in Cairo, Egypt. Figure 14.a shows a Masjid in Location 1 oriented to Makkah direction, namely Qabalah, however Figure 14.b shows church facing east in location 1 also. Figure 14.c displays two adjacent worship buildings worship buildings, which consist of

masjid oriented to Qabalah by facing South East direction, and church facing East. The Location 2 is located at one of the famous district in East Cairo zone, in Egypt.

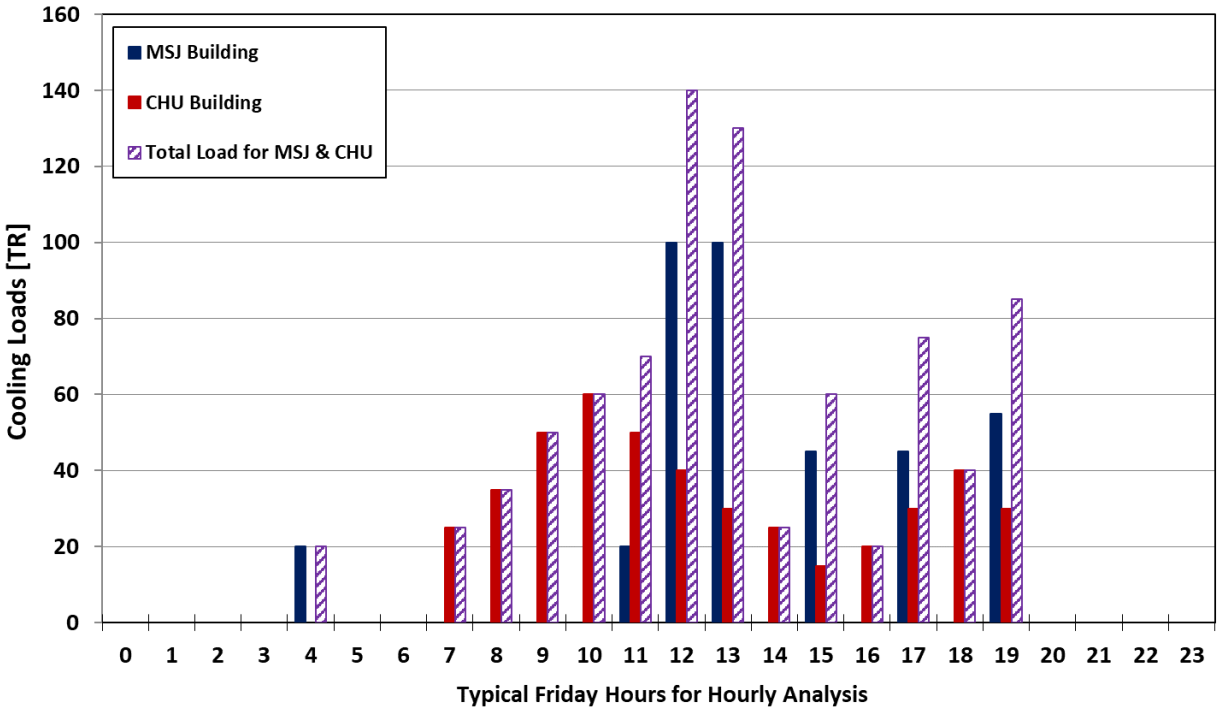

a

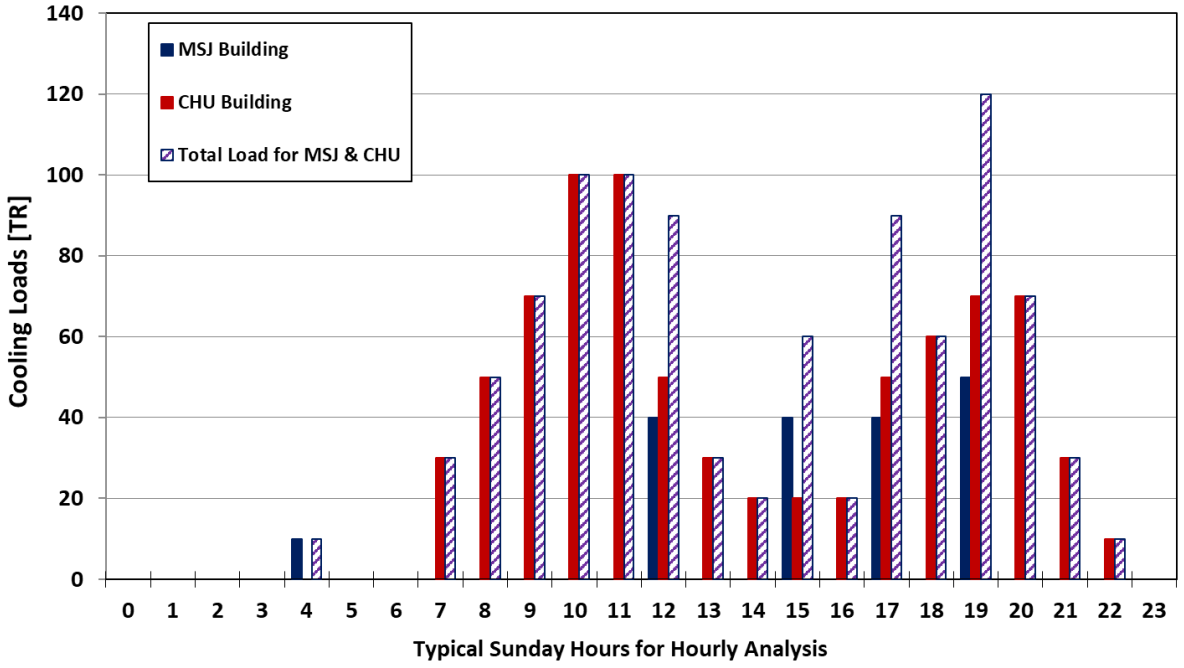

b

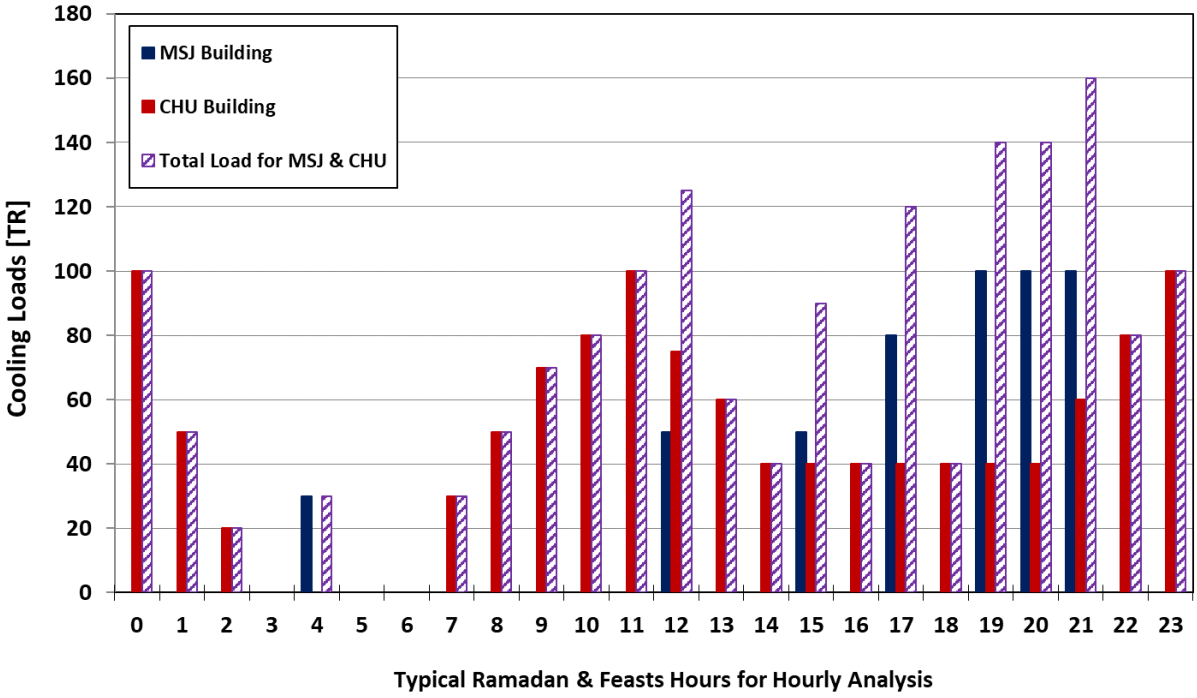

c

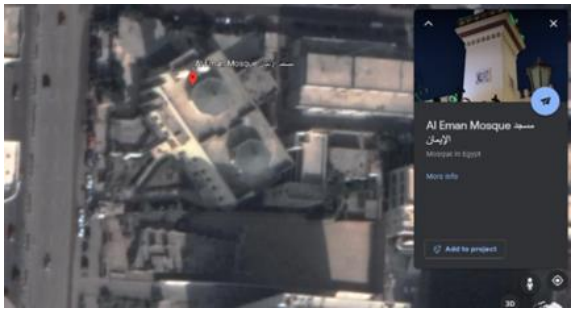

d **e**

f

Figure 15: Cooling Load profiles for Masjid, Church and total for both buildings for different typical holidays of Fridays, Sundays, Ramadan and Feasts, a) Cooling Load profiles for Typical Friday in July beside satellite view

for Masjid in Cairo, b) Cooling Load profiles for Typical Sunday in July beside satellite view for Church in Cairo facing east at the morning, and c) Cooling Load profiles for typical Ramadan/feast day (3rd May 2021) beside satellite view for existing arrangements consist of Masjid and Church buildings in Cairo.

6. Conclusion and Recommendations

The current research concludes several concluding remarks as following besides suggestions for future work.

- Experimental work using scale down modelling can be successfully used to generate a deep insight views for air distribution and thermal comfort for worshipers inside different architecture designs for worship buildings consists of church and masjid, either located in upper Egypt weather conditions, or at the North of Egypt. Different operating conditions can be also predicted based on the worshiper observed behavior and occupancy levels, which directly affects the cooling load demand inside the worship building.
- CFD modeling can be accepted to simulate the air distribution with different configurations, to get the optimal air distribution inside different architecture designs for worship buildings consists of church and masjid. CFD modeling should be carefully validated before depending on these results, which greatly affected by the assumed boundary conditions and operating range. Different operating conditions can be numerically investigated to predict the thermal behavior to ensure the thermal comfort for worshipers inside worship building under different air distribution design configurations and under different loading conditions, to take into consideration the worshipers occupancy levels, which directly affects the cooling load demand either inside masjids or inside churches.
- Combining two different buildings with different applications results in a reduction in the design load. The present work has highlighted a common example in Egypt which is the coexisting of churches and masjids (mosques) in the same neighborhood. The cooling load analysis detailed in this paper has shown that the combined load should not exceed 60% of the individual load of each building in the worst scenario (occurrence of common feasts days in July). Future planed urban designs adopting the construction of both worship building in the same block should consider the construction of a common cooling system for both buildings as an energy reduction solution to meet the comfort needed under such discreet activities buildings.

The suggestions for future work are to perform a CFD numerical investigation for church buildings similar to those presented in this current article for masjid building with two different configuration based on the air distribution arrangements.

Authors ORCID

Tarek A. Mouneer https://orcid.org/ 0000-0001-7781-1803

Mohamed H. Aly https://orcid.org/0000-0003-4892-0976

Ehab M. Mina https://orcid.org/0000-0001-6402-3920

References

[1] D.K. Bohl, T.L. Hanna, A.C. Scott, J.D. Moyer, S.G. Hedden, Sustainble development goals report Egypt 2030. Josef Korbel School of international studies university of Denver 2018. https://pardee.du.edu/sites/default/files/SDG_Report_Egypt_2030+(1).pdf.

[2] P.O. Fanger, Assessment of man's thermal comfort in practice. Br J Ind Med 1973; 30: 313–324. Google Scholar, Medline.

[3] P.O. Fanger, Thermal comfort: analysis and applications in environmental engineering. Appl Ergon 1970; 3: 181–181.

[4] P. Ricciardi, C. Buratti, Thermal comfort in the Fraschini theatre (Pavia, Italy): correlation between data from questionnaires, measurements, and mathematical model. Energy Build 2015; 99: 243–252.

[5] P. Ricciardi, A.Ziletti, C. Buratti, Evaluation of thermal comfort in an historical Italian opera theatre by the calculation of the neutral comfort temperature. Energy Build 2016; 102: 116–127.

[6] Q.J. Kwong, N.M. Adam, B.B. Sahari, Thermal comfort assessment and potential for energy efficiency enhancement in modern tropical buildings: A review, Energy Build. 68 (2014) 547–557. https://doi.org/10.1016/j.enbuild.2013.09.034.

[7] I.M. Budaiwi, An approach to investigate and remedy thermal-comfort problems in buildings, Building and Environment, Volume 42, Issue 5, 2007, Pages 2124-2131, ISSN 0360-1323. https://doi.org/10.1016/j.buildenv.2006.03.010.

[8] E. Mushtaha, O. Helmi, Impact of building forms on thermal performance and thermal comfort conditions in religious buildings in hot climates: a case study in Sharjah city International Journal of Sustainable Energy Volume 36, 2017 - Issue 10.

[9] T.J. Terrill, B.P. Rasmussen, An evaluation of HVAC energy usage and occupant comfort in religious facilities, Energy Build. 128 (2016) 224–235. https://doi.org/10.1016/j.enbuild.2016.06.078.

[10] A. Hayati, M. Mattsson, M. Sandberg, Single-sided ventilation through external doors: Measurements and model evaluation in five historical churches, Energy Build. 141 (2017) 114–124. https://doi.org/10.1016/j.enbuild.2017.02.034.

[11] C.M. Muñoz-González, A.L. León-Rodríguez, J. Navarro-Casas, Air conditioning and passive environmental techniques in historic churches in Mediterranean climate. A proposed method to assess damage risk and thermal comfort pre-intervention, simulation-based, Energy Build. 130 (2016) 567–577. https://doi.org/10.1016/j.enbuild.2016.08.078.

[12] F. Frasca, E. Verticchio, C. Cornaro, A.M. Siani, Performance assessment of hygrothermal modelling for diagnostics and conservation in an Italian historical church, Building and Environment, Volume 193, 2021, 107672, ISSN 0360-1323, https://doi.org/10.1016/j.buildenv.2021.107672.

[13] F.E. Turcanu, M. Verdes, I. Serbanoiu, Churches Heating: The Optimum Balance Between Cost Management and Thermal Comfort, Procedia Technol. 22 (2016) 821–828. https://doi.org/10.1016/j.protcy.2016.01.055.

[14] R.C. Vella, F.J.R. Martinez, C. Yousif, D. Gatt, A study of thermal comfort in naturally ventilated churches in a Mediterranean climate, Energy Build. 213 (2020) 109843. https://doi.org/10.1016/j.enbuild.2020.109843.

[15] N. Aste, S. Della Torre, R.S. Adhikari, M. Buzzetti, C. Del Pero, F. Leonforte, M. Manfren, Sustainable church heating: The Basilica di Collemaggio case-study, Energy Build. 116 (2016) 218–231. https://doi.org/10.1016/j.enbuild.2016.01.008

[16] M. Wessberg, T. Broström, T. Vyhlidal, ScienceDirect ScienceDirect ScienceDirect A method to determine heating power and heat up time for intermittent on District Heating and Cooling heating of churches the feasibility of using the heat a long-term district heat demand forecast, Energy Procedia. 132 (2017) 915–920. https://doi.org/10.1016/j.egypro.2017.09.720.

[17] G. Woroniak, J. Piotrowska-woroniak, Effects of pollution reduction and energy consumption reduction in small churches in Drohiczyn community, Energy Build. 72 (2014) 51–61. https://doi.org/10.1016/j.enbuild.2013.12.048.

[18] T. de Rubeis, I. Nardi, M. Muttillo, D. Paoletti, The restoration of severely damaged churches – Implications and opportunities on cultural heritage conservation, thermal comfort and energy efficiency, J. Cult. Herit. 43 (2020) 186–203. https://doi.org/10.1016/j.culher.2019.11.008.

[19] L. Wang, Y. Qu, Influence of Chinese and Western Culture on Modern Church Architecture in Yan'an Area, Journal of Building Construction and Planning Research, Vol.03 No.04 (2015) 180–188, DOI: 10.4236/jbcpr.2015.34018

[20] S.A.R. Saeed, Thermal comfort requirements in hot dry regions with special reference to Riyadh Part 2: for Friday prayer. Int J Ambient Energy 1996; 17: 17–21.

[21] M.S. Al-homoud, A.A. Abdou, I.M. Budaiwi, Assessment of monitored energy use and thermal comfort conditions in mosques in hot-humid climates, 41 (2009) 607–614. https://doi.org/10.1016/j.enbuild.2008.12.005.

[22] F.F. Al-Ajmi, Thermal comfort in air-conditioned mosques in the dry desert climate. Build Environ 2010; 45: 2407–2413.

[23] F.H. Abdullah, N.H.A. Majid, R. Othman, Defining Issue of Thermal Comfort Control through Urban Mosque Façade Design, Procedia - Soc. Behav. Sci. 234 (2016) 416–423. https://doi.org/10.1016/j.sbspro.2016.10.259.

[24] A.B. Atmaca, G.Z. Gedik, Energy & Buildings Evaluation of mosques in terms of thermal comfort and energy consumption in a temperate-humid climate, Energy Build. 195 (2019) 195–204. https://doi.org/10.1016/j.enbuild.2019.04.044.

[25] N.A. Azmi, S.H. Ibrahim, A comprehensive review on thermal performance and envelope thermal design of mosque buildings, Build. Environ. 185 (2020) 107305. https://doi.org/10.1016/j.buildenv.2020.107305.

[26] I.M. Budaiwi, A.A. Abdou, M.S. Al-Homoud, Envelope retrofit and air-conditioning operational strategies for reduced energy consumption in mosques in hot climates. Build Simul 2013; 6: 33–50.

[27] A.A. Abdou, M.S. Al-Homoud, I.M. Budaiwi, Mosque energy performance, part I: energy audit and use trends based on the analysis of utility billing data. J King Abdulaziz Univ: Eng Sci 2005; 16: 165–184.

[28] I.M. Budaiwi, Envelope thermal design for energy savings in mosques in hot-humid climate. J Build Perform Simul 2010; 4: 49–61.

[29] S. Ray, S. Sadaba, L. Leung, Intelligently controlled naturally ventilated mosque – a case study of applying design tools throughout the design process, International Journal of Ventilation Volume 16, 2017 - Issue 2: Breakthrough of natural and hybrid ventilative cooling technologies: strategies, applications and case studies.

[30] A.B. Atmaca, G.Z. Gedik, Determination of thermal comfort of religious buildings by measurement and survey methods: Examples of mosques in a temperate-humid climate, J. Build. Eng. 30 (2020) 101246. https://doi.org/10.1016/j.jobe.2020.101246.

[31] N.A. Azmi, M. Arıcı, A. Baharun, A review on the factors influencing energy efficiency of mosque buildings, J. Clean. Prod. 292 (2021). https://doi.org/10.1016/j.jclepro.2021.126010.

[32] A. Elkhateeb, S. Eldakdoky, The acoustics of Mamluk masjids: A case study of Iwan-type masjids in Cairo, Appl. Acoust. 178 (2021) 107988. https://doi.org/10.1016/j.apacoust.2021.107988.

[33] E. Farrag, Architecture of mosques and Islamic centers in Non-Muslim context, Alexandria Eng. J. 56 (2017) 613–620. https://doi.org/10.1016/j.aej.2017.08.001.

[34] S.G.S. Shah, Doctors in Pakistan denounce opening of mosques for congregational prayers during Ramadan amid the COVID-19 pandemic: Correspondence, Int. J. Surg. 79 (2020) 40–41. https://doi.org/10.1016/j.ijsu.2020.05.006.

[35] D. Bolster, R.E. Hershberger, R.J. Donnelly, Dynamic similarity, the dimensionless science, (2011).

[36] Y.K. Yi, N. Feng, Dynamic integration between building energy simulation (BES) and computational fluid dynamics (CFD) simulation for building exterior surface. Build Simul 2013; 6: 297–308.

[37] Y. Fan, T. Hayashi, K. Ito, Coupled simulation of BES-CFD and performance assessment of energy recovery ventilation system for office model. J Central South Univ 2012; 19: 633–638.

[38] Y. Fan, K. Ito, Integrated building energy computational fluid dynamics simulation for estimating the energy-saving effect of energy recovery ventilator with CO2 demand-controlled ventilation system in office space. Indoor Built Environ 2014; 23: 785–803. Google Scholar, SAGE Journals, ISI.

[39] D.N. Sørensen, P.V. Nielsen, Quality control of computational fluid dynamics in indoor environments. Indoor Air 2003; 13: 2–17.

[40] A.A. Youssef, E.M. Mina, A.R. ElBaz, R.N. AbdelMessih, Studying comfort in a room with cold air system using computational fluid dynamics, Ain Shams Eng. J. 9 (2018) 1753–1762. https://doi.org/10.1016/j.asej.2016.07.005.